Applications of Infrared Spectroscopy to Biochemical, Food and Agricultural Process

Atsushi Hashimoto and Takaharu Kameoka

Division of Sustainable Resource Sciences, Graduate School of Bioresources,

Mie University, Tsu, Mie, Japan

Abstract: Integrated investigations on the infrared spectroscopic characteristics of metabolites and on applications of infrared spectroscopy to foodstuff production, food processing and tasting are described. As the important metabolites, saccharides, which play very important roles in various functions are located in the central position of the metabolic pathways, were selected, and the spectral features the saccharides and related materials are discussed. Additionally, the applications of such a spectral analysis to the monitoring of the enzyme reaction and the sugar metabolic processes, which are the main materials in food processing, are described. Furthermore, the studies on the spectroscopic measurements during the cultivation of agricultural products as foodstuffs and in the tasting as the final quality evaluation of foods are represented. These results suggest that infrared spectroscopy could be very effective for evaluating foodstuff production and the tasting of the processed foods and that the applied topics should provide fundamental information about the spectral behavior of the metabolites and bioproducts.

Keywords: infrared spectroscopy, metabolites, agriculture, food processing, tasting, sugar, monitoring, metabolic kinetics, enzyme reaction, fermentation

INTRODUCTION

People are becoming more health-conscious, therefore, it is necessary to produce sustainable and high quality foodstuffs and processed foods. Recently, food safety and guaranteed of food brands have become more serious subjects of foodstuff production and the marketing of processed foods. Quality management (such as following the ISO 9000 family), food safety management (such as following the ISO 22000 family) and environmental management (such as following the ISO 14000 family) during cultivation and the processing of the foodstuffs are important in order to consistently produce high quality products for the marketing. Combination of Good Agricultural Practices (GAP) and Good Manufacturing Practice (GMP) are becoming the new factors in all comprehensive management plans in the agricultural fields and food industries. For such a purpose, food traceability systems are actively being developed using advanced information and communication technology (ICT). However, in many cases, there is a lack of evidence of the food qualities based on the sensing data.

Therefore, the quality evaluation and control of foods and agricultural products based on the actual sensing data are required in order to consistently manufacture high quality products. For food safety, quality sensing from the foodstuff production to the

tasting of foods is needed and should be simple, non-destructive, simultaneous, rapid, qualitative and quantitative. In addition, the usefulness of the measured data for software evaluations is also required. The optical and spectroscopic methods could theoretically satisfy their requirements. Furthermore, most of the recent remarkable non-destructive measurements of food and agricultural products are based on optical and spectroscopic techniques. Especially, the appearance sensing of them using visible rays (1) and the internal component measurements by infrared (IR) spectroscopy (2) are popular and widely utilized. The former is divided into the shape and color measurements, and the three-dimensional shape analysis and full-color analysis are common techniques. The latter is roughly divided into near and mid-infrared (NIR and MIR) spectroscopic applications. The NIR applications are very extensive in agricultural and food processing research areas (2-8) along with the chemometric techniques such as Partial Least-Squares (PLS) and Principal Component Regression (PCR) methods. On the other hand, there are many theories on the fundamental vibration modes of various functional groups for MIR spectroscopy and linear regression analysis at a specified wavenumber would be effective and useful in many cases. However, the strong absorption of the MIR rays by the water inside foods is a problem. The spectroscopic method using a Fourier transform infrared (FT-IR) spectrometer equipped with an attenuated total reflection (ATR) (9, 10) accessory (FT-IR/ATR) has substantial potential as a quantitative tool for such measurements (11, 12).

The quality of foods and agricultural products is influenced by not only the molecular structure of the components, but also the interactions between the molecule

and its environment. This review focuses on the applications of IR spectroscopy for quality evaluations and control through the foodstuff production to the tasting of the processed foods based on the fundamental subjects which are mainly our studies, since the IR spectrum could be reflected by such factors and most of the component have very active in the IR region.

First, this review describes the spectral features of metabolites, especially monosaccharides and disaccharides, such as glucose and sucrose, which play very important roles in various functions and are located in the central part of the metabolic pathways. Also, the saccharides are very important components that influence the quality of the agricultural products and the food tastes. Moreover, the studies on the spectroscopic measurements during the food processing and cultivation of agricultural products as foodstuffs are explained. Control and evaluation of the quality of agricultural products are very important in order to make stable and suitable cultivation management practices, and the monitoring of the enzyme reaction and the sugar metabolic processes as the point materials in the food processing. Furthermore, the tasting as the final quality evaluation of foods using IR spectroscopy is described.

INFRARED SPECTROSCOPIC CHARACTERISTICS OF METABOLITES

Saccharides in Aqueous Solution

Saccharides, based on the degree of polymerization, can be classified as monosaccharides, disaccharides, oligosaccharides, and polysaccharides. Each of the four

classes of saccharides plays an important role in biological products. For example, the polysaccharides are stored fuels (starch) and structural materials (cellulose), and the oligosaccharides have various functions in biological activities. The monosaccharides and disaccharides, such as glucose and sucrose, occupy a central position in the sugar metabolic bioprocess. Among these saccharides, the monosaccharides and disaccharides are important biomolecules (13). In addition, water is a major constituent of the bioproducts and foods; and it is important to determine the interaction patterns between the saccharide molecules and water. This is especially important for the saccharides-water interaction, when the disaccharide, trehalose, substitutes for water and maintains the life of organisms exposed to an arid environment (14). The interaction between the saccharides and water is closely related to their constituent monosaccharides, types of glycosidic bonds, and degree of polymerization (15, 16).

The MIR spectra of monosaccharides in aqueous solutions (0.30 M) are shown in Figure 1 (17), which was obtained by subtracting the spectra of the solvents multiplied by a factor calculated using the density of the solvents and molar concentration of the solutions. Therefore, the absorption of saccharides and interactions between them and the solvents were observed in the spectra as shown in Figure 1. Different spectral patterns were found in the fingerprint region from 1200 to 950 cm^{-1} for each of the monosaccharides in the aqueous solutions, indicating that the interaction between the monosaccharides and solvents depends on the structure of the saccharides and on the type of solvents.

The fingerprint region represents the characteristics of the C-C, C-H, C-O and

O-H vibration motions of the saccharides. As a result, many peaks were observed in the region and overlapped each other in a complex manner. Among the carbohydrates, glucose in the aqueous solution has been extensively studied by the infrared spectroscopic method (18-23). Especially, the absorption band at 1150 cm^{-1} has been identified as a characteristic of the pyranose sugars (18) while the band at 1100 cm^{-1} has been assigned to the combined vibration modes including C-C, C-O and C-OH (19). The band at 1080 cm^{-1} is typical of the bending vibration mode of C-1-H (18, 19). The band at 1030 cm^{-1} corresponds to the C-4-OH vibration (20). Furthermore, for fructose in the aqueous solution, there is a C-1-OH vibration mode at 1060 cm^{-1} (22). We also observed the above-mentioned absorption bands in the spectra of mannose, galactose and talose in the aqueous solutions. However, in the same and diluted concentrations, the monosaccharides structure consisting of a pyranose or franose ring and the C-OH orientation affected the absorption intensity rather than the wavenumber shift.

The MIR spectra of the disaccharides in the aqueous solutions (0.15 M) are shown in Figure 2 (17). The spectra were extracted using the same method as that of the monosaccharides spectra. Various spectral patterns were found in the fingerprint region for each disaccharide. In the spectra of trehalose and maltose, the absorption band at 1030 cm^{-1} corresponds to the C-4-OH vibration of the glucose residue (21). The band in the glucose spectrum such as 1080 cm^{-1}, assigned to the bending vibration mode of C-1-H, was observed in the spectra of the disaccharides in the aqueous solutions. The absorption bands were also observed in the spectra of the other ones that consist of two glucoses in the aqueous solutions. Furthermore, for sucrose in an aqueous solution, there is a C-1-OH

vibration of the fructose residue at 1060 cm^{-1} (21). The above-mentioned absorption bands were also observed in the spectra of the others consisting of glucose and fructose. The glycosidic linkage position and the constituent monosaccharides had effects on the absorption intensity rather than on the wavenumber shift. The characteristic spectral pattern in this region and sharp peaks at 995 cm^{-1}, assigned to the vibration mode of the glycosidic linkage (21), were observed for trehalose and sucrose containing the same type of glycosidic bond in the aqueous solution. This indicates that, regardless of their constituent monosaccharides, the same type of glycosidic bonds, as trehalose, have similar effects on the disaccharides-water interactions. Based on the above discussions, Kanou *et al*. indicated the significant influences of the glycosidic linkage position and the constituent monosaccharides on the infrared spectral characteristics of the disaccharides in the aqueous solutions that could be determined using the FT-IR/ATR method (17).

Saccharides in Aqueous Solutions with Alkaline Metal Salts

For the hydration of electrolytes, such as Na and K, their importance in a biological medium is as well known as that of the saccharides. The Na^+ and K^+ ions are involved in the membrane potential change and, very likely, their distribution. The rate of their transfer across the receptor membrane is essential to the chemoreception in biological products (13). Additionally, since water is the major constituent of the bioproducts, the interaction between the saccharide molecules, salts and water is one of the most important factors for the organisms. This subsection focuses on both the chlorides of alkaline metals including Na and K as salts and glucose which plays a very

important role in the organisms.

The MIR spectra of water and a 2.0 M glucose solution with various concentrations of NaCl are shown in Figure 3 (24). The OH stretching vibration region from 3800 to 2800 cm^{-1} and the OH bending vibration region from 1850 to 1350 cm^{-1} showed that the spectral pattern continuously changed when the concentration of NaCl increased, similar to the spectra of the aqueous solutions of NaCl,. Additionally, the spectral pattern changed in the fingerprint region from 1200 to 950 cm^{-1} for glucose. These spectral features were also found in the spectra of 2.0 M glucose solutions containing LiCl, KCl, RbCl, and CsCl. As mentioned above, in the OH stretching vibration region from 3800 to 2800 cm^{-1}, we clearly observed the influence of chlorides on the water and solution for each chloride. However, in this region, the OH stretching vibration of both the glucose molecules and the hydrogen bonding between the glucose, NaCl and water overlapped. Therefore, we focused our attention on the fingerprint region (1200 to 950 cm^{-1}) of glucose.

Figure 4 indicates the subtracted spectra of glucose in the NaCl aqueous solutions (24). Since we used the factors of water and NaCl, the absorbance of the glucose includes the interaction between the glucose, NaCl and water. The varying spectral pattern was found in the region from 1200 to 950 cm^{-1} for each NaCl concentration. It was found that the glucose, NaCl-water interaction depended on the concentration of NaCl, because the glucose concentration was fixed 2.0 M. To correlate those interactions with the concentrations, we subtracted the spectrum of glucose in the aqueous solution without NaCl from the spectra of those with NaCl as shown in Figure 5.

Therefore, these spectra exhibited the influence of solvents consist of NaCl and water on glucose. Figure 5 shows that the spectral pattern continuously changed and that the absorbance of the functional groups increased with the increase in the NaCl concentrations (24). These results indicated that the influence of solvents on the functional groups of the glucose molecules increased with those of the NaCl concentrations. In the fingerprint region, there are many peaks due to the C-C, C-H, C-O and O-H vibration motions of the saccharides, which complicatedly overlap each other (Figures 4 and 5). From comparison between Figures 4 and 5, it was found that the influence of the NaCl concentration on each functional group of glucose for the above-mentioned absorption bands shifted to lower wavenumbers. These spectral features were also observed in the spectra of the 2.0 M glucose solutions with LiCl, KCl, RbCl, and CsCl.

Ionic Dissociative Metabolites

As the pH value varies everywhere in a biological system, the ionic dissociative conditions of the metabolic components should be noticed. The application of spectroscopy, especially in the infrared region, to such measurements is desirable as a high potential implementation. Incidentally, the spectroscopic method using an FT-IR/ATR method provides substantial potential as a quantitative tool based on the molecular structure and on the interactions between the molecule and its environment.

The pH-dependency of the MIR spectra in an aqueous solution of the organic dissociative materials in the metabolic pathway, such as saccharide phosphates (G6P,

F6P), adenosine and its phosphates (ATP, ADP AMP), was studied (25). The series of molar absorbance spectra for these reagents were obtained in the pH range from about 2 to 11 for the FT-IR/ATR method using a horizontal diamond internal reflection element (IRE).

The ATR spectrum of the ionic dissociative material in the aqueous solutions significantly changes with pH. In Figure 6 (25), the molar absorbance spectra of the G6P aqueous solution at different pHs are presented. The phosphoric group contained in G6P gives the sharp peak at 980 cm^{-1}. A similar pH dependency of the results shown in Figure 6 was observed for the other ionic dissociative metabolites (25, 26). The above spectral behavior was analyzed as follows.

The pH-dependency of the ATR absorbance spectrum for an ionic dissociative material XH_n in an aqueous solution could be explained by the equilibrium shift among the ionic dissociation components (ionic species).

$$XH_n \xleftrightarrow{pK_1} XH_{n-1}^{-} + H^+ \xleftrightarrow{pK_2} XH_{n-2}^{2-} + 2H^+ \xleftrightarrow{pK_3} \cdots \xleftrightarrow{pK_n} X^{n-} + nH^+ \quad (1)$$

Henceforth, the spectrum of each ionic species was assumed to be not affected by the hydrogen ion concentration and satisfies the spectral additivity for the ionic species. The spectrum from which the pure water spectrum was subtracted can then be decomposed by the assumed spectra of the ionic species, as follows:

$$Abs(\nu, \mathrm{pH}) = \sum_{i=0}^{n} c_i(\mathrm{pH}) Abs_i(\nu) \quad (2)$$

where, ν denotes the wavenumber, $Abs(\nu, \mathrm{pH})$ is the subtracted spectrum per unit molar of the reagent. $c_{,i}(\mathrm{pH})$ is the fraction of the reagent's total concentration for the *i*-th ionic

species with the charge -*i*, and $Abs_{,i}(\nu)$ is the molar absorbance spectra of the *i*-th components. According to the dissociation equilibrium theory, the fraction for the *i*-th component $c_{,i}$ (pH) can be expressed as a function of pH with the parameters of the dissociation constants pK_i.

$$
\begin{aligned}
c_0(\mathrm{pH}) &= \frac{[XH_n]}{C} = \frac{1}{1+10^{\mathrm{pH}-pK_1}+10^{\mathrm{pH}-pK_1}10^{\mathrm{pH}-pK_2}+\cdots+10^{\mathrm{pH}-pK_1}\cdots10^{\mathrm{pH}-pK_n}} \\
c_1(\mathrm{pH}) &= \frac{[XH^{-}_{n-1}]}{C} = \frac{10^{\mathrm{pH}-pK_1}}{1+10^{\mathrm{pH}-pK_1}+10^{\mathrm{pH}-pK_1}10^{\mathrm{pH}-pK_2}+\cdots+10^{\mathrm{pH}-pK_1}\cdots10^{\mathrm{pH}-pK_n}} \\
c_2(\mathrm{pH}) &= \frac{[XH^{2-}_{n-2}]}{C} = \frac{10^{\mathrm{pH}-pK_1}10^{\mathrm{pH}-pK_2}}{1+10^{\mathrm{pH}-pK_1}+10^{\mathrm{pH}-pK_1}10^{\mathrm{pH}-pK_2}+\cdots+10^{\mathrm{pH}-pK_1}\cdots10^{\mathrm{pH}-pK_n}} \\
&\vdots
\end{aligned}
\qquad (3)
$$

Here, *C* denotes the total concentration of the reagent in the aqueous solution. The dissociation constants pK_i of the reagents were found in the literature (27, 28).

By performing the multiple linear regression analysis using the model formula in Equations (2) and (3), the molar absorbance spectra of ionic species for G6P, as well as the corresponding monosaccharide, glucose, were obtained as shown in Figure 7 (25). Two ionic species for G6P were obtained in the measured pH range, $G6P^-$ and $G6P^{2-}$. By comparing the ionic species of G6P with glucose, we observed that the characteristic absorption of glucose in the fingerprint region was inherited by the ionic species of G6P, especially the -1 charged ion; $G6P^-$. On the contrary, the sharp peaks at 1080 cm^{-1} and 990 cm^{-1} observed in the orthophosphoric acid (25) are apparently identified in the absorbance spectrum of the -2 charged ion; $G6P^{2-}$.

Using the molar absorbance spectra of the ionic species of the dissociative materials obtained in this procedure, the molar absorbance spectra of the dissociative

materials in aqueous solution at any pH could be reconstructed. In Figure 8 (25), the synthesized spectra for G6P at pH 5.78 and 7.10 are compared with the observed spectra when prepared at these pH values. The agreement of these spectra was fairly good. This suggests that it will be possible to construct a quantification system for the concentrations of the organic dissociative materials at varying pH.

APPLICATION TO AGRICULTURAL FIELDS

Measurement of Multiple Modes of Nitrogen

Valuable information on plant nutrition needs to address not only the nutrient contents, but also their balance in the plant organs over the entire period of plant and harvest product development. A quantitative monitoring should be carried out by a simple to use, non-destructive, simultaneous, and rapid method. In addition, the measured data need to be retrieved for future simulations using various modeling software programs. Application of X-ray fluorescence (XRF) for the chemical element measurement and MIR spectroscopy for the organic component measurement shows a high potential for process implementation in the entire supply chain (29-32). Incidentally, for developing portable spectrometers, both spectroscopic methods provide substantial potential as quantitative tools in the field to analyze the plant vigor. This subsection describes the development process of a simultaneous and quantitative method for evaluating the elements and the plant vigor using MIR spectroscopy (33). The MIR information on the nitrogen in different modes was studied in the tomato leaf for obtaining on-site data of the

nutritional status of the plant.

Figure 9 shows the MIR spectra of the fresh tomato leaf and the leaf models impregnated with some variations in the concentrations of proteinic and nitrate mixed nitrogen solutions (33). The spectra of the leaf models had the spectral features very similar to the fresh tomato leaf. Weak peaks are observed at around 1350 cm^{-1} where the absorption band of the NO stretching mode of the nitric functional groups could exist. Furthermore, absorption peaks of the amino functional groups at 1650 and 1550 cm^{-1} could not be easily recognized, since the very high peak due to the OH bending of water was observed around this band.

The MIR spectra of the leaf models after the spectral subtraction of the leaf model impregnated by water provided the MIR spectroscopic information about the components under question. At 1350 cm^{-1}, the order of the absorbance versus that of the nitric acid concentration of the leaf model were measurable (Figure 10 (33)). As a result, the nitrate nitrogen content in the leaf model could be determined by the MIR spectroscopic method. Furthermore, the simultaneous determination of the nitrate and proteinic nitrogen would be possible using the ratio of the nitrate nitrogen content to the proteinic one.

These results show the significant potential of obtaining the nutrient information on the nitrogen in the adapted calibration models by applying the spectroscopic method. Additionally, the spectral information could also be associated with the other information related to the plant vigor (34), especially with the image information obtained by a digital camera (35-38) in an easy and cheap way.

Measurements of Pesticide Residues and Classification

The consumer's concern for food safety has caused the strongest need for a rapid and accurate measurement method of pesticide residues in foods, such as the agriculture products that are eaten raw. However, the conventional methods, such as chromatography, are not feasible, because these methods take several hours or, in some cases, several days to measure the pesticide residues. Infrared spectroscopy has been used for the rapid, non-destructive and easy measurements of pesticide residues on agricultural products and the classification for a safe food source supply. Kurt *et al.* developed the FT-IR/ATR method to detect three kinds of bactericides (39). Figure 11 shows the spectra of lettuce with or without daconil, oxine-copper and topsin-M (40). Significant differences in the spectral features are observed. Furthermore, Ishizawa *et al.* suggested that the FT-IR/ATR method could have the potential to be a rapid and accurate system for the measurement of the pesticide residues (40-42). Also, his group proposed the Fourier transform infrared diffuse reflectance spectroscopy (FT-IR-DRS) measurement system to achieve this aim by using pattern recognition (43, 44).

APPLICATION TO FOOD PROCESS

Biggs reported the MIR spectroscopic quantification of milk fat, protein, and lactose in milk in 1967 (45), and this was the first scientific report about food analysis using the MIR spectroscopic method. Since then, there have been many approaches for food analysis using the IR spectroscopic methods (for example; 46-48). In this subsection, the applications of such spectral analyses to the monitoring of the enzyme reaction and

the sugar metabolic processes, which are the central materials in food process, are represented.

Quantification System of Ionic Dissociative Materials

In cells, every enzyme reaction proceeds in conjunction with and in parallel to some of the other enzyme reactions. In addition, the kinetic parameters *in vivo* may be different from those *in vitro*. Furthermore, each metabolite could choose the most suitable molecular structure for its physical, chemical and biological environments, such as pH. Some experimental approaches to determine these factors were reported (for example; 49). For such experiments, it is very important that not only the metabolite content components, but also their molecular structures in the metabolic reaction system are non-destructively and simultaneously monitored in real time. Moreover, as the pH value varies everywhere in the biological system, the ionic dissociative conditions of the metabolites should be determined in these analyses. In this and the following sections, the simultaneous quantification method of the concentrations of ionic dissociative materials and pH value and the continuous and non-destructive monitoring of the enzyme reaction process associated with the ionic dissociative metabolites are described. The enzyme reaction from G6P to fructose 6-phosphate (F6P) with D-glucose-6-phosphate ketol-isomerase (PGI) was studied (50-52). This enzyme reaction occurs at the beginning of the glycolytic pathway, which would administer the overall metabolism, and might be appreciated as one of the most important biological reaction in experimental and computational metabolic engineering.

Every wavenumber corresponding to the negative peak of the second derivative spectra of all the ionic components was assembled. Among the assembled peaks of the second derivative spectra, we selected ones corresponding to the peaks of the absorbance spectra. Additionally, the wavenumbers corresponding to lower determination coefficients for the MLR analysis in the above spectral extraction (25) were removed. We then selected the 24 wavenumbers corresponding to the peaks of the absorbance spectra from 1186 to 926 cm^{-1} in which the metabolite spectra would not be affected by the enzyme.

Again, the MLR analysis about the relationship between the second derivation values at each selected wavenumber and the concentration of the dissociation component in the G6P-F6P-Tris mixture solutions was performed for verification (53).

$$d^2Abs(\nu_n) = \sum_k \sum_i \mathrm{C}_{k,i} d^2Abs_{k,i}(\nu_n) \qquad (4)$$

where, ν_n denotes the selected wavenumber. For the seven samples prepared for the verification, the concentrations of the dissociation components $C_{k,i}$ were calculated. We evaluated the pH value of the G6P-F6P-Tris mixture solution using the relation of the dissociation equilibrium for the calculated concentration of the dissociation components of the Tris that could control the pH value as the buffer. With the calculated pH value and $C_{k,i}$ values, we quantified the G6P, F6P and Tris concentrations using the dissociation equilibrium relation.

A comparison of the calculated values with the actual pH value and G6P, F6P and Tris concentrations is shown in Figure 12 (50). The very good agreement between the actual and the estimated values were observed in all cases. Their correlation coefficients are all higher than 0.997, and we determined a sufficient accuracy

In this quantification system, the concentrations of the dissociation components of the Tris buffer were used to calculate the pH of the sample. In other words, the dissociative reagent itself acted as a kind of pH indicator. Especially, materials used for buffer typically shift the ionic dissociation equilibrium around its buffering range. Since the reaction mixture for the enzyme assay usually contains a buffer, it is an advantage of our quantification system that the buffering materials itself can be utilized for the pH indicator. Moreover, the infrared spectrum of each dissociation component of the dissociative material calculated by the quantification system includes much information about the molecular structure of biochemical substance in the metabolic systems. This information will be significant for the analysis of the enzymatic dynamics during the intracellular reactions.

Monitoring of Enzyme Reaction Associating with Ionic Dissociative Metabolites

The simultaneous quantification method of ionic dissociative material concentrations and pH values in the mixed solutions was applied to continuously and non-destructively monitor the enzyme reaction process from G6P to F6P with PGI in a constructed reactor equipped with an FT-IR system.

The time changes in the second derivative spectra of the reactant components during the enzyme reaction are partly indicated in Figure 13 (52). The spectral changes during the enzyme reaction process were very slight, and moderate spectral movements were observed. This suggests that the G6P as the substrate would be spectroscopically quite similar to the F6P as the product in this pH region. Such a spectral similarity would

be common to the enzyme reaction in the metabolic pathways and cycles.

We applied the developed quantification method to the time behavior of the MIR spectral information of the reactant (Figure 13) obtained by the reactor system. Figure 14 shows the time courses of the quantified metabolite concentrations and pH value during the enzyme reaction (52). The pK values used in the quantification process were evaluated at 313 K (27, 28). This evaluation method of the pK values provided almost the same accuracy for the MIR spectroscopic determination of the metabolite concentrations and pH value at 313 K (data not shown) as that at 298 K presented in Figure 12.

As shown in Figures 14(a) and (b), the G6P and F6P concentrations successively decreased and increased with the reaction time, respectively. Both of them finally reached a plateau stage where they were very roughly around 15 mM. In addition, the fluctuations in the time courses of the quantified concentrations of G6P, F6P and Tris were observed, though the calculated pH value was stable throughout the enzyme reaction (Figure 14(c)) and the sample temperature was stable at 312.9 to 313.5 K (data not shown). Since the agitation was not carried out during the enzyme reaction in this study, the stagnation of the reactant on the IRE of the ATR accessory might cause fluctuations in the quantification results. This is the principle problem, but it would be ease to alleviate the fluctuation by mechanically improving the agitation conditions.

The G6P and F6P concentrations were also calculated by applying a simple Michaelis-Menten type model with the acceptive kinetic parameters to the reaction conditions. The calculated results are also displayed in Figures 14(a) and (b). No significant difference was observed between the time behaviors of the concentrations

calculated by the MIR spectroscopic quantification method and evaluated by the simple calculation. Additionally, the Tris concentration determined by the MIR spectroscopic method was roughly constant throughout the enzyme reaction, and the values were almost the same as the actual one (Figure 14(c)). Moreover, the evaluated pH value in the quantification agreed with the one measured by a pH meter (Figure 14(c)). These results could suggest the acceptability of the developed method for the actual metabolic reactions. Consequently, it could be possible to monitor the actual bioprocess in real-time on-/in-line by attaching the IRE crystal equipped with the optical fiber and the simple spectrometer.

Metabolite Content Determination in Plant Cell Culture Medium

Fermented bioproducts are widely utilized in various fields, such as the food and agricultural industries. During the fermentation process, the monitoring and the judgments of the fermentation state are very important for the successful production. Alcohol and lactic acid fermentation play very important roles in food processing. Saccharides, such as glucose, fructose and sucrose, are the key carbon sources, and continuous monitoring using the infrared spectroscopic information is desirable (54, 55). In this and the next subsection, example studies of the plant cell cultivation (56-61) and the lactic acid fermentation monitoring are described, respectively (62).

Suspending cells in the liquid medium could sense the medium information and the states of the other cells and uptake the nutrition components from the outside. The components of such a medium in which the cells are involved in the biochemical process

are always changing.

This subsection describes the potential of the spectroscopic method by comparison with a high-performance liquid chromatography (HPLC) method and applying the developed method to the simultaneous measurement of the ethanol content with the sugar ones in the liquid culture media with suspended rice (*Oryza sativa* L., Japonica, cv. Nipponbare: R2S) and tabaccum (*Nicotiana tabacum* cv. Bright Yellow No.2: TBY-2) cells, respectively.

Figure 15 shows the ATR spectra of sucrose, glucose, fructose and ethanol in the R2S media, which were obtained after the spectral subtraction of water, in the fingerprint region from 1300 to 900 cm^{-1} (59). For the sugars, there were many peaks, such as the CO and C-OH stretching modes, which complicatedly overlap each other (11, 12, 18), especially in the region from 1150 to 950 cm^{-1}. In addition, ethanol had a significant sharp peak around 1045 cm^{-1}, which did not overlap the sugar peaks mentioned above. Thus, each sugar and ethanol in the medium with its spectral pattern can be identified in this region. The peaks around 1055, 1036, 1065 and 1045 cm^{-1} mainly characterize the sucrose, glucose, fructose and ethanol spectra, respectively (59).

Focusing on the above wavenumbers, we made calibration curves between the absorbance and the metabolite concentrations in the media and the following straight line fit all the curves.

$$A_i(\nu) = a_i(\nu)C_i + b_i(\nu) \qquad (5)$$

where $A_i(\nu)$ and C_i are, respectively, the absorbance and the concentration of the metabolite (i) at the wavenumber (ν). The slope, $a_i(\nu)$, of the straight line relates to the

types of metabolites and the value of $b_i(\nu)$ may theoretically show the absorbance of the medium without the metabolite.

For the calibration curves of the metabolites in the R2S medium, an excellent linearity was observed for each metabolite at each wavenumber. Also, the correlation coefficient for ethanol at 1045 cm^{-1} where the ethanol spectrum has the sharpest and most stainable peak as shown in Figure 15, is 0.999. In addition, those for sugars at that wavenumber are all higher than 0.999. Moreover, the $b_i(\nu)$ values at the four wavenumbers for all the metabolites are equal to the experimental values of the absorbance of the medium without the metabolite. These results indicate that the *b* values can be used only as a function of the wavenumber.

Since the above results experimentally suggest that the FT-IR/ATR method may have a potential for the metabolite content determination in the R2S medium, the MIR spectroscopic metabolite content determination in the R2S medium was performed using the Bouguer-Beer's law based on the assumption of the spectral additivity as follows (56, 59):

$$A(\nu) = \sum_i a_i(\nu) C_i + b(\nu) \quad (6)$$

Equation (6) is rewritten as a matrix expression.

$$\begin{pmatrix} A_{1055} \\ A_{1035} \\ A_{1065} \\ A_{1045} \end{pmatrix} = \begin{pmatrix} a_{suc,1055} & a_{glc,1055} & a_{fru,1055} & a_{EtOH,1055} \\ a_{suc,1035} & a_{glc,1035} & a_{fru,1035} & a_{EtOH,1035} \\ a_{suc,1065} & a_{glc,1065} & a_{fru,1065} & a_{EtOH,1065} \\ a_{suc,1045} & a_{glc,1045} & a_{fru,1045} & a_{EtOH,1045} \end{pmatrix} \begin{pmatrix} C_{suc} \\ C_{glc} \\ C_{fru} \\ C_{EtOH} \end{pmatrix} + \begin{pmatrix} b_{1055} \\ b_{1035} \\ b_{1065} \\ b_{1045} \end{pmatrix} \quad (7)$$

where the left subscripts suc, glc, fru and EtOH, respectively, mean sucrose, glucose, fructose and ethanol. The right subscripts indicate the wavenumbers. Moreover, Equation

(7) has the other expression (Equation (8)).

$$\begin{pmatrix} C_{suc} \\ C_{glc} \\ C_{fru} \\ C_{EtOH} \end{pmatrix} = \begin{pmatrix} a_{suc,1055} & a_{glc,1055} & a_{fru,1055} & a_{EtOH,1055} \\ a_{suc,1035} & a_{glc,1035} & a_{fru,1035} & a_{EtOH,1035} \\ a_{suc,1065} & a_{glc,1065} & a_{fru,1065} & a_{EtOH,1065} \\ a_{suc,1045} & a_{glc,1045} & a_{fru,1045} & a_{EtOH,1045} \end{pmatrix}^{-1} \begin{pmatrix} A_{1055} - b_{1055} \\ A_{1035} - b_{1035} \\ A_{1065} - b_{1065} \\ A_{1045} - b_{1045} \end{pmatrix} \quad (8)$$

In the comparison of the metabolite contents in the R2S medium determined by the above MIR spectroscopic or HPLC method, which is one of the present standard methods, with the actual ones, an excellent agreement between the actual and estimated metabolite contents for both analytical methods is obtained. Their correlation coefficients are all higher than 0.99. This may suggest that the FT-IR/ATR spectroscopy is applicable for the content determination of not only the sugars, but also ethanol (the metabolic product) as an accurate method. In addition, it takes ten or twenty minutes for the HPLC measurement while the ATR spectrum was obtained within one minute. Furthermore, the MIR spectrum provides the information about all components having an infrared activity, though the HPLC data provide only information for each component after the pre-treatment for the HPLC measurement. Hence, the MIR spectroscopy has a higher performance than the other analytical methods for monitoring the cultivation process from the viewpoint of the kinetic metabolic analysis.

Figure 16 is a comparison of the quantification results of the metabolites in the R2S medium during the rice cell cultivation using the MIR spectroscopic method with those using the HPLC method (59). Very good agreements for the sugar and ethanol contents between both were observed and the validity of the application of the simple and rapid MIR spectroscopic methods to the simultaneous determination of the nutrient and productive content during the rice cell cultivation were experimentally confirmed. Hence

these results indicate that the sugar consumption and ethanol production behavior during cultivation could be continuously observed using the spectra in the R2S culture medium for the rice cell cultivation by the FT-IR/ATR method.

In addition, for the MS medium with suspended TBY-2 cells, which produce little ethanol during cultivation, the sugar content determined by the MIR spectroscopic method based on the ethanol existence in the medium indicated a better accuracy than that determined by the previous method neglecting the absorption by ethanol in the medium (56). Therefore, the spectroscopic method described in this paper could be developed as a technique to analyze the overall kinetic metabolism of the suspension plant cells because the FT-IR/ATR method has the potential to theoretically determine most of the metabolites including the ionic dissociative materials (25, 50).

Yogurt Fermentation

The lactic acid fermentation was performed under the different conditions of the media and the starter concentration in order to examine the FT-IR/ATR method for the medium component measurements. Yogurts were made from the mixture of the medium (reconstituted skimmed milk) and yogurt starter. The Skim milk powder consisted of 4.48% moisture, 0.72% fat, 34.46% protein, 7.77% mineral and 52.77% lactose, and the starter contained *Streptococcus thermophilus* and *Lactobacillus burgaricus* strains. The media with the suspended sample strains were soaked in a thermostated water bath at 310 K for 6 h.

Figure 17 shows an example of the spectral evolution of the yogurt-fermentation

sample between 1200 and 800 cm^{-1} (62), where the spectrum characterizes the sugars. These spectra were characterized by the peaks at 1075 and 1041 cm^{-1} resulting from the ether CO vibration and C-OH vibration of the lactose, respectively (11). Since the peak at 1075 cm^{-1} was the most stable, the absorbance of this peak was used in this study. A two-point baseline correction with the absorbances of 1184 and 960 cm^{-1} was done to the absorbance of the peak at 1075 cm^{-1}. Based on the results shown in Figure 17, the acidity change during the fermentation was examined. The linear relationships between the corrected absorbance at 1075 cm^{-1} were obtained for all the medium concentrations, and all correlation coefficients were greater than 0.998. The slopes of the line were all -0.036, which meant that the efficiency of the lactose metabolism to lactic acid was constant throughout the fermentation process.

Additionally, the peaks from the protein dynamically changed with the fermentation time as shown in Figure 18 (62), which represented the structure behavior of proteins in the medium due to the pH change based on the lactic acid production during fermentation. This suggested that the FT-IR/ATR method could be applicable not only to evaluate the lactic acidity based on the lactose content in the fermentation medium, but also to monitor the change in the protein structure.

DEVELOPMENT OF TASTING ROBOT

This subsection describes an artificial sense of taste and the world's first “tasting robot” (63-65), which was developed by collaboration of NEC System Technologies, Ltd.,

and Mie University under the support by The New Energy and Industrial Technology Development Organization (NEDO) for the Robot Project: Prototype Robot Exhibition at EXPO 2005 AICHI, JAPAN (66).

Lendl *et al.* proposed the “optical-tongue” concept based on the spectroscopic information of foods (67). We have developed an optical-tongue with an IR sensor. It is attached to a personal robot, PaPeRo (68). The optical-tongue is the integration of the IR spectroscopic technologies with pattern recognition technologies.

Concept of Tasting Robot

The robot could be expected to have at least three major potential when it has a sense of taste. The first potential is to qualitatively and quantitatively analyze the major components in a food sample such as sugar and fat. Because a human doesn't have this ability, the robot with this ability can provide useful advice to a human in various situations. The second potential is to express the similar taste feelings of a food sample to a human's. Humans have various words and phrases to express their feelings of taste; “I am sure you will like this wine and it matches well with Sushi”. A robot with this ability can become a critique of food and a human can enjoy a discussion about food or drink with the robot. The last potential is to identify the names of food products. It requires a human with special skills and training. If the robot has the ability, a human can have his/her own sommelier and obtain useful and interesting advice. In addition, if the name of a food product is spectroscopically identified, its main components and average contents are then estimated by referring to the literature.

There are two approaches to provide information about the sense of taste by analyzing the food and its components. One is the use of transducers of a sensor composed of lipids immobilized with polyvinyl chloride. The sensor has the concept of "global selectivity" which is the ability to classify enormous amounts of chemical substances into basic taste groups such as saltiness, sourness, bitterness, umami and sweetness (69). This approach is effective to realize the second and third abilities defined in the previous subsection. The size of the sensor is now similar to a desktop PC.

The other one is the use of the spectroscopic fingerprint information of foods; i.e., an optical-tongue technique (11, 12, 17, 64, 69-73). It has the advantage of requiring a very short measurement time. This approach is then effective to realize the first and third ability defined in the previous subsection. In addition, the size of the sensors is getting smaller. Furthermore, the hand-held sensors are already commercialized, and it is now possible to attach a sensor to a personal robot.

The tasting robot has an architecture consisting of three modules (Natural language dialog module, Taste analysis module with an IR sensor and its controller, the Advice generation module) as shown in Figure 19 (63, 64). We also decided to use a commercial robot software development tool, RoboStudio (74). It provides the natural language dialog module. By using RoboStudio, a human designer just defines a set of scenarios which describes a sequence of conversation dialogs between a human and a robot.

We assumed that the tasting robot will be placed in a dining kitchen or on a dining table and taste foods and drinks. Therefore, its size must be similar to a thermos

bottle. PaPeRo is also a small partner robot. It is about 0.5 m tall with speech recognition and generation functions. Because it satisfies our requirements, we decided to use PaPeRo by attaching an arm with an IR sensor as shown in Figure 20 (63, 64).

Spectroscopic Fingerprints of Foods

It is known that each food has different IR spectral characteristics; i.e., the spectroscopic fingerprints. For example, the differences in the spectral pattern among the varieties and of the intensities of the peaks characterizing each type are observed. We could then understand the quantitative spectroscopic fingerprint information of foods. Therefore, there are two independent methods for analyzing a food spectrum as indicated in Figure 21 (63, 64). Both of them are stored in the taste analysis module shown in Figure 19.

The spectroscopic quantification was performed by studying the concentration dependencies of the spectra of the main components such as the sugar, acid and fat in a food sample (an example is shown in Figure 22 (65, 71)) and by making the calibration curves. The quantification method was quite acceptable for a comparatively simple foodstuff, but it was difficult to complete the perfect calibration curves for the chemically and structurally complicated foods.

On the other hand, the pattern recognition techniques were introduced to identify food names. The IR spectroscopic fingerprint information of various food samples were accumulated and stored with their food names in a pattern database. If a food sample is given, its spectrum pattern is compared with the stored spectrum patterns and the

distances are calculated. A food name with the closest distance is assumed to be identical to the food sample.

The basic algorithm of the food identification analysis consists of two steps. Step-1 selects a set of wavenumbers which are effective for calculating the distances between the spectra of a sample food and the stored one. Because a spectrum pattern covers a wide range of wavenumbers (wavelength), the calculated distances at all points over the wavenumbers is very time-consuming and ineffective. Step 2 uses a canonical correlation analysis (66) where its input variables are the absorbance ratio at selected wavenumbers of a spectrum, and its output variable is the food name.

Challenge to Develop Sommelier Robot in the Future

One of the most difficult foods we evaluated was wine. The spectral differences among the tested wines were strikingly smaller than those among the other types of foods. In order for the robot to be able to achieve the ability to differentiate wine, we made several improvements as follows.

(a) Improvements were made to the resolution using an ATR accessory.

(b) Discrimination is conducted by focusing on the automatic extracted point.

(c) The robot is now equipped with the ability to ask questions in order to determine a customer's wine preferences like a human sommelier. In this subsection, the focus is on the spectroscopic analysis upon extraction of the wine fingerprints for the identification (65, 73).

Figure 23 represents the absorbance spectra of red and white wines (65, 73),

water and ethanol aqueous solutions. The spectral patterns of the wines show the qualitative and quantitative agreements with those of the ethanol aqueous solution, especially in the wavenumber ranges of 3100 to 2800 cm^{-1} and of 1500 to 900 cm^{-1}. The influence of the ethanol, which is the major component of the wine, on the spectral information is too significant to identify a brand of wine based on the absorbance. The spectral extraction of the wine components except for ethanol and water was then examined.

By studying the spectral characteristics of the correlation coefficients between the second derivatives of the ethanol in the aqueous solution and the concentrations and the vibrational modes of the peaks characterizing them, the multiple linear regression analysis model for the ethanol content determination using the second derivative values at 1981, 1419, and 1085 cm^{-1} was constructed. The ethanol contents estimated for the alcoholic drinks consistently agreed with those obtained by a high-performance liquid chromatography method. The ethanol spectrum in the wine, which was calculated on the basis of the estimated ethanol content in consideration of the interactions between the ethanol and water, was subtracted from the wine spectrum. Moreover, by subtracting the water spectrum from the above one, the spectral information of the wine components other than ethanol and water could be experimentally and simulatively extracted. The absorption bands characterizing the wine components other than ethanol and water are then clearly observed and the fingerprint information is able to be confirmed. Based on the above improvements, the robot could identify several tens of wine brands (Figure 24 (65, 73)).

The above method is an important step in the developments of the quality and taste of wines based on the IR spectroscopic fingerprint, and the robot development was selected by the TIME magazine as one of the Best Inventions of 2006 (75) and in the 2008 Guinness Book as the first wine-bot (76). However, in order to develop it for various fields, there is a time when the improvement becomes necessary in the future. We will continue to develop it in these fields.

CONCLUDING REMARKS

Recent developments in FT-IR and accessories have provided many kinds of sampling techniques and new analyzing methods. These are very important for acquiring the IR spectral information of wet bioproducts with complicated molecular and geometrical structures and to better understand of them. This review mainly focuses on the spectral features of saccharides, which play very important roles in various functions, and occupy the center parts of the metabolic pathways. Additionally, the applications of such a spectral analysis to the monitoring of the enzyme reaction and the sugar metabolic processes, which are the main materials in food processing are described in this manuscript. Furthermore, the studies of the spectroscopic measurements during the cultivation of agricultural products as foodstuffs and in the tasting as the final quality evaluation of foods are represented. These results suggest that infrared spectroscopy could be very effective from the foodstuff production to the tasting of the processed foods and that the applied topics should provide the fundamental information about the spectral

behavior of the metabolites and the bioproducts. For the complicated materials in agriculture and food processing, we need to understand the spectral features not only for the peak analysis, but also about the influences of the geometric structures (77-84).

As for the recent progress in IR imaging, which is related to the food and agricultural fields (85-91), the microscopic and macro imaging and remote sensing are being actively studied. However, for more progress in the IR imaging, the spectral understandings are consequently quite required and important studies. Moreover, the relationship between the infrared and terahertz spectra (92-96) might be one of the challenging topics related to this review (97). Therefore, the fundamental and canonical spectroscopic methods described in this paper could be in conjunction with the imaging techniques in various scales and terahertz spectroscopy and have the potential to be a new research field in food and agricultural engineering because of the affinities of the spectra for software use.

Acknowledgements

We thank Dr. Mikihito Kanou, Assistant Professor of Mie University, and Dr. Kenichi Nakanishi, Associate Professor of Mie University, for their valuable insights and numerous productive discussions. We also thank Dr. Tao Pan, Professor of Jinan University, Mr. Atsushi Yamanaka, PhD student of Mie University, and Mr. Hisanori Mori, former PhD student of Mie University, for their collaborative works and experimental support.

References

1. Sagara, Y. (1996) Recent Developments of Sorting and Grading System for Fruits and Vegetables by Optical Sensing. *Journal of the Japanese Society for Food Science and Technology*, 43: 215.
2. Kazarian, S. G., Chan, K. L. A., Maquet, V., Boccaccini, A. R. (2004) Characterisation of Bioactive and Resorbable Polylactide/Bioglasss Composites by FTIR Spectroscopic Imaging. *Biomaterials*, 25: 3931.
3. Nosal, W. H., Thompson, D. W., Yan, L., Sarkar, S., Subramanian, A., Woollam, J. A. (2005) UV–VIS–Infrared Optical and AFM Study of Spin-Cast Chitosan Films. *Colloids and Surface* B, 43: 131.
4. Sugiyama, J. (1999) Visualization of Sugar Content in the Flesh of a Melon by Near-Infrared Imaging. *Journal of Agriculture and Food Chemistry*, 47: 2715.
5. Tsuta, M., Sugiyama, J., Sagara, Y. (2002) Near-Infrared Imaging Spectroscopy Based on Sugar Absorption Band for Melons. *Journal of Agriculture and Food Chemistry*, 50: 48.
6. Raab, T. K., Vogel, J. P. (2004) Ecological and Agricultural Applications of Synchrotron IR Microscopy. *Infrared Physics and Technology*, 45: 393.
7. Osborn, B. G., Fearn, T. (1986) *Near Infrared Specteroscopy in Food Analysis*; John Wiley: New York.
8. Siesler, H. W., Ozaki, Y., Kawata, S., Heise, H. M. (2002) *Near-Infrared Spectroscopy-Principles, Instruments, Applications*; WILEY-VCH: Weinheim.

9. Harrick, N. J. (1967) *Internal Reflection Spectroscopy*; Harrick Scientific Corporation: New York.
10. Mirabella, F. M., Harrick, N. J. (1985) *Internal Reflection Spectroscopy: Review and Supplement*; Harrick Scientific Corporation: New York
11. Kameoka, T., Okuda, T., Hashimoto, A., Noro, A., Shiinoki, Y., Ito, K. (1998) FT-IR Analysis of Sugars in Aqueous Solution Using ATR Method. *Journal of Japanese Society of Food Science and Technology*, 45: 192.
12. Kameoka, T., Okuda, T., Hashimoto, A., Noro, A., Shiinoki, Y., Ito, K. (1998) A Rapid FT-IR/ATR Method for Sugar Content Determination in Food. *Journal of Japanese Society of Food Science and Technology* 45: 199.
13. Nelson, D. L., Cox, M. M. (2000) *Lehninger Principles of Biochemistry*, 3rd ed., Worth Publishers: New York.
14. Akao, K., Okubo, Y., Asakawa, N., Inoue, Y., Sakurai, M. (2001) Infrared Spectroscopic Study on the Properties of the Anhydrous Form II of Trehalose. Implications for the Functional Mechanism of Trehalose as a Biostabilizer. *Carbohydrate Research*, 334: 233.
15. Kanou, M., Nakanishi, K., Hashimoto, A, Kameoka, T. (2003) Infrared Spectroscopic Analysis of Disaccharides in Aqueous Solutions. *Journal of Japanese Society of Food Science and Technology*, 50: 57.
16. Kanou, M., Hashimoto, A., Motonaga, Y., Kameoka, T. (2001) Determination of Polymerization Degree of Maltooligosaccharides by FT-IR/ATR Spectroscopy. *Journal of Japanese Society of Food Science and Technology*, 48: 401.

17. Kanou, M., Nakanishi, K., Hashimoto, A., Kameoka, T. (2005) Influences of Monosaccharides and Its Glycosidic Linkage on Infrared Spectral Characteristics of Disaccharides in Aqueous Solutions. *Applied Spectroscopy*, 59: 885.
18. Cael, J., Koenig, J. L., Blackwell, J. (1974) Infrared and Raman Spectroscopy of Carbohydrates: Part IV. Identification of Configuration- and Conformation-Sensitive Modes for D-Glucose by Normal Coordinate Analysis. *Carbohydrate Research*, 32: 79.
19. Vasko, P. D., Blackwell, J., Koenig, J. L. (1972) Infrared and Raman Spectroscopy of Carbohydrates: Part II: Normal Coordinate Analysis of α-glucose. *Carbohydrate Research*, 23: 407.
20. Vasko, P. D., Blackwell, J., Koenig, J. L. (1971) Infrared and Raman Spectroscopy of Carbohydrates: Part I: Identification of O-H and C-H-Related Vibrational Modes for D-glucose, Maltose, Cellobiose, and Dextran by Deuterium-Substitution Methods. *Carbohydrate Research*, 19: 297.
21. Kacurakova, M., Mathlouthi, M. (1996) FTIR and Laser-Raman Spectra of Oligosaccharides in Water: Characterization of the Glycosidic Bond. *Carbohydrate Research*, 284: 145.
22. Zhbankov, R. G., Andrianov, V. M., Marchewka, M. K. (1997) Fourier Transform IR and Raman Spectroscopy and Structure of Carbohydrates. *Journal of Molecular Structure*, 436: 637.
23. Back, D. M., Polavarapu, P. L. (1983) Fourier-Transform Infrared Spectroscopy of Sugars. Structural Changes in Aqueous Solutions. *Carbohydrate Research*, 121: 308.

24. Kanou, M., Yamanaka, A., Hashimoto, A., Kameoka, T. (2004) Infrared Spectroscopic Analysis of Saccharides in Aqueous Solutions with Alkaline Metal Salts. In *Proceedings of 10th Asian Pacific Confederation of Chemical Engineering Conference*, 3P-01-056.
25. Nakanishi, K., Hashimoto, A., Kanou, M., Pan, T., Kameoka, T. (2003) Mid-Infrared Spectroscopic Measurement of Ionic Dissociative Materials in Metabolic Pathway. *Applied Spectroscopy*, 57: 1510.
26. Hashimoto, A., Asada, K., Matsuo, T., Teraura, C., Yamamura, T., Yasui, K., Yamanaka, A., Kanou, M., Kameoka, T. (2005) Mid-Infrared Spectroscopic Characteristics of Glycine in Aqueous Solution. In *Proceedings of 7th Asia-Pacific Conference of Biochemical Engineering*, CUR-06.
27. Martell, A. E., Smith, R. M. (1974-1989) *Critical Stability Constants*, Plenum Press: New York.
28. Chemical Society of Japan (Ed.) (1993) *Kagaku Binrann (Handbook of Chemistry)*, 4th ed., Maruzen: Tokyo.
29. Hashimoto, A., Niwa, T., Yamamura, T., Suehara, K., Kanou, M., Kameoka, T., Kumon, T., Hosoi, K. (2006) X-Ray Fluorescent and Mid-Infrared Spectroscopic Analysis of Tomato Leaves. In *SICE-ICASE International Joint Conference 2006*, pp.3359-3562.
30. Hayashi, N., Hashimoto, A., Suehara, K., Kanou, M., Kameoka, T., Kumon, T., Hosoi, K. (2007) X-Ray Fluorescent and Mid-Infrared Spectroscopic Measurements of Vigor Information of Tomato Plant. In *Proceedings of SICE Annual Conference*

2007, pp.220-223.

31. Hashimoto, A., Niwa, T., Rahman, M., Nakanishi, K., Kameoka, T., Kumon, T., Hosoi, K. (2004) X-Ray Fluorescent Spectroscopic Analysis of Tomato Leaf. In *Proceedings of AFITA/WCCA2004 Joint Congress on IT in Agriculture*, Zazueta, F., Ninomiya, S., Chitradorn, R. (eds.), pp.874-879.
32. Myint, W. W., Motonaga, Y., Hashimoto, A., Kameoka, T. (2001) Respiratory Characteristics of Stored Tomato (Part 1) -Comparison of Desicator and Film Storage-, *Journal of the Japanese Society of Agricultural Machinery*, 63(2): 60.
33. Hashimoto, A., Niwa, T., Yamamura, T., Rahman, M., Nakanishi, K., Kameoka, T., Kumon, T., Hosoi, K. (2005) X-Ray Fluorescent and Mid-Infrared Spectroscopic Measurement of Leaf Model. In *Proceedings of EFITA/WCCA 2005 Joint Conference*, pp.252-259.
34. Oka, M., Kameoka, T., Hashimoto, A., Nakanishi, K., Itou, R., Mishima, T., Shono, H., Taki, H., Uchio, F., Saito, Y., Ishizawa, H., Motonaga, Y., Hoshi, T., Iguchi, N., Mizoguchi, M., Goto, E., Harada, M., Ninomiya, S., Hirafuji, M., Fukatsu, T. (2004) Application of Some Sensing Techniques for Evaluating a Condition of a Coffee Tree. In *Proceedings of AFITA/WCCA2004 Joint Congress on IT in Agriculture*, Zazueta, F., Ninomiya, S., Chitradorn, R. (eds.), pp. 470-476.
35. Motonaga, Y., Kondou, H., Hashimoto, A., Kameoka, T. (2004) A Method of Making Digital Fruit Color Charts for Cultivation Management and Quality Control. *Journal of Food, Agriculture and Environment*, 2: 160.
36. Hashimoto, A., Yasui, K., Takahashi, M., Yonekura, S., Hirozumi, T., Mishima, T., Ito,

R., Suehara, K., Kameoka, T. (2006) Remote Monitoring of Color of Agricultural Products in the Field Using a Digital Camera and the Field Server. In *4th World Congress of Computers in Agriculture and Natural Resources*, pp.66-71.

37. Hashimoto, A., Kondou, H., Motonaga, Y., Kitamura, H., Nakanishi, K., Kameoka, T. (2002) Evaluation of Tree Vigor by Digital Camera based on Fruit Color and Leaf Shape. In *Proceedings of 1st World Congress of Computers in Agriculture and Natural Resources*, pp.70-77.
38. Hashimoto, A., Ito, R., Iguchi, N., Nakanishi, K., Mishima, T., Hirozumi, T., Hirafuji, M., Ninomiya, S., Kameoka, T. (2007) An Integrated Field Monitoring System for Sustainable and High-Quality Production of Agricultural Products Based on BIX Concept with Field Server. In *Proceedings of The 2007 International Symposium on Applications and the Internet* (CD-version).
39. Kurtz, G., Bellon, V. (1991) Pesticide Measurement on Fruits and Vegetable Surfaces. In *Proceedings of the 1991 IFT Annual Meeting*, p.180.
40. Ishizawa, H., Nakamura, M., Toba, E., Iwasaki, T. (1996) Optical Measurement of Multielement of Pesticide Residues. *SICE Transactions*, 33: 54.
41. Ishizawa, H., Toba, E., Okamura, T., Tokoo, R. (1996) Validation of a Measurement System for Pesticide Residues on Vegetables Based on Optical Measurement. *Journal of Robotics and Mechatronics*, 8: 203.
42. Ishizawa, H., Toba, E., Nakamura, M. (2000) Nondestructive Measurement of Insecticide Residues in Chinese Cabbage Based on Infrared ATR Spectroscopy. *Journal of the Japanese Society of Agricultural machinery*, 62(6): 136.

43. Ishizawa, H., Nishimatsu, T., Toba, E. (2001) Measurement of Pesticide Residues in Food Based on Diffuse Reflectance IR Spectroscopy. In *18th IEEE Instrumentation and Measurement Technology Conference*, pp.884-887.
44. Ishizawa, H., Nishimatsu, T., Toba, E. (1998) Semiquantatuve At-line Measurement System for Multiresidues of Pesticide in Food Based on the ATR Spectroscopy. In *15th IEEE Instrumentation and Measurement Technology Conference*, pp.675-678.
45. Biggs, D. A. (1967) Milk Analysis with Infrared Milk Analyzer. *Journal of Dairy Science*, 50: 799.
46. van de Voort, F. R., Kermasha, S., Smith, J. P., Mills, B. L., Ng-Kwai-Hang, K. F. (1987) A Study of the Stability of Record Performance Milk Samples for Infrared Milk Analysis. *Journal of Dairy Science*, 70: 1515.
47. Darwish, G. S., van de Voort, F. R., Smith; J. P. (1989) Proximate Analysis of Fish Tissue by Mid-Infrared Transmission Spectroscopy. *Canadian Journal of Fisheries and Aquatic Science*, 46: 644.
48. Hashimoto, A. (2006) Development of Infrared Radiative and Spectroscopic Applications to Food Processing. *Japan Journal Food Engineering*, 7: 61.
49. Flores, S., Gosset, G., Flores, N., de Graaf, A. A., Bolivar, F. (2002) Analysis of Carbon Metabolism in Escherichia coli Strain with an Inactivate Phosphotransferase System by 13C Labeling and NMR Spectroscopy. *Metabolic Engineering*, 4: 124.
50. Pan, T., Hashimoto, A., Kanou, M., Nakanishi, K., Kameoka, T. (2003) Development of a Quantification System of Ionic Dissociative Materials in the Glycolytic Pathway Using an FT-IR/ATR Method. *Bioprocess and Biosystems Engineering*, 26: 133.

51. Pan, T., Hashimoto, A., Kanou, M., Nakanishi, K., Kameoka, T. (2004) Mid-Infrared Spectroscopic Quantification of Ionic Dissociative Metabolites Based on Three Spectral Extraction Methods. *Japan Journal of Food Engineering*, 5: 23.
52. Hashimoto, A., Pan, T., Kanou, M., Nakanishi, K., Kameoka, T. (2005) Mid-Infrared Spectroscopic Monitoring of Enzyme Reaction Associating with Ionic Dissociative Metabolites. In *Computer Applications in Biotechnology 2004*, pp.375-380; Elsevier Science: Oxford.
53. Nakanishi, K., Pan, T., Hashimoto, A., Kameoka, T. (2002) Quantification System of Ionic Dissociative Materials in Glycolytic Pathway Using Infrared Spectroscopic Information. In *Proceedings of the 6th SCI*, Vol. XIII, pp.268-273.
54. Alberti, J. C., Phillips, J. C., Fink, D. J., Wacasz, F. M. (1985) Off-Line Monitoring of Fermentation Samples by FTIR/ATR: A Feasibility Study for Real-Time Process Control. *Biotechnology and Bioengineering Symposium*, 15: 689.
55. Fayolle, P., Picque, D., Perret, B., Latrille, E., Corrieu, G. (1996) Determination of Major Compounds Alcoholic Fermentation by Middle-Infrared Spectroscopy: Study of Temperature Effects and Calibration Method. Applied Spectroscopy, 50: 1325.
56. Hashimoto, A., Kameoka, T. (2000) Mid-Infrared Spectroscopic Determination of Sugar Contents in Plant-Cell Culture Media Using an ATR Method. *Applied Spectroscopy*, 54: 1005.
57. Hashimoto, A., Nakanishi, K., Motonaga, Y., Kameoka, T. (2001) Sugar Metabolic Analysis of Suspensions of Plant Cells Using an FT-IR/ATR Method. *Biotechnology Progress*, 17: 560.

58. Hashimoto, A., Yamanaka, A., Kanou, M., Nahar, F., Kameoka, T. (2003) Effects of Pre-Cultivation on Sugar Metabolic Kinetics of Suspension Plant Cells Measured by Mid-Infrared Spectroscopy. *Journal of Food, Agriculture and Environment*, 1: 168.
59. Hashimoto, A., Yamanaka, A., Kanou, M., Nakanishi, K., Kameoka, T. (2005) Simple and Rapid Determination of Metabolite Content in Plant Cell Culture Medium Using an FT-IR/ATR Method. *Bioprocess and Biosystems Engineering*, 27: 115.
60. Yamanaka, A., Hashimoto, A., Kanou, M., Kameoka, T. (2005) MIR Spectroscopic Analysis on Sugar Metabolic and Ethanol Productive Kinetics of Suspension TBY-2 and Rice Cells Pre-Cultured in Various Media. *Bioprocess and Biosystems Engineering*, 27: 125.
61. Yamanaka, A., Hashimoto, A., Matsuo, T., Kanou, M., Suehara, K., Kameoka, T. (2007) Analysis of Kinetic Uptake Phenomena of Monosaccharide and Disaccharide by Suspension TBY-2 Cells Using an FT-IR/ATR Method. *Bioprocess and Biosystems Engineering*, 30: 457.
62. Hashimoto, A., Kameoka, T., Shiinoki, Y., Ito, K. (1998) Mid-Infrared Spectroscopic Determination of Sugar Contents in Culture Media. In *Computer Applications in Biotechnology 1998*, pp.411-416; Elsevier Science Ltd.: Oxford (1998)
63. Shimazu, H., Kobayashi, K., Hashimoto, A., Kameoka, T. (2005) Tasting Robot: a Personal Robot with an Optical-Tongue. In *Proceedings of 36th International Symposium on Robotics*.
64. Shimazu, H., Kobayashi, K., Hashimoto, A., Kameoka, T. (2007) Tasting Robot with

an Optical Tongue: Real Time Examining and Advice Giving on Food and Drink. In *Human Interface, Part I, HCII 2007*, M.J. Smith, G. Salvendy (eds.), pp.950-957; Springer-Verlag: Berlin Heidelberg.

65. Hashimoto, A., Kameoka, T., Kanou, M., Suehara, K., Shimazu, H., Kobayashi, K. (2006) Development of a Personal Robot with a Sense of Taste by Infrared Spectroscopy. In *Proceedings of the 22nd NIR Forum*, pp.67-70.
66. Japan Association for the 2005 World Exposition (2005) http://www.expo2005.or.jp/en/robot/robot_project_02.html.
67. Edelmann, A., Lendl, B. (2002) Toward the Optical Tongue: Flow-Through Sensing of Tannin-Protein Interactions Based on FTIR Spectroscopy. *Journal of American Chemical Society*, 124: 14741.
68. Fujita, Y. (2002) Personal Robot PaPeRo. *Journal of Robotics and Mechatronics*, 14: 60.
69. Toko, K. (2001) *Kansei Bio Sensor*, Asakura Shoten: Tokyo.
70. Hashimoto, A., Mori, H. Kanou, M. Yamanaka, A., Kameoka, T. (2004) Mid-Infrared Spectroscopic Analysis on Brewed Coffee Characteristics. In *Proceedings of 10th Asian Pacific Confederation of Chemical Engineering Conference*, 3P-01-068.
71. Hashimoto, A., Takada, S., Motonaga, Y., Nakanishi, K., Kameoka, T. (2002) Spectroscopic Determination of Acid and Sugar Content in Fruit Juice. In *Control Applications in Post-harvest and Processing Technology 2001*, pp.209-214; Elsevier Science Ltd.: Oxford.
72. Hashimoto, A., Kameoka, T. (1997) Penetration of Infrared Radiation within a

Vegetable Model. *Food Science and Technology, International, Tokyo*, 3: 373.

73. Hashimoto, A., Kameoka, T., Kanou, M., Suehara, K., Ehara, H., Shimazu, H., Kobayashi, K. (2006) Infrared Spectroscopic Sensing of Food and Agricultural Information. In *Proceedings of 2006 Annual Conference of The Illuminating Engineering Institute of Japan*, pp.278-279.
74. RoboStudio Web page (2007) http://www.necst.co.jp/product/robot/.
75. TIME (2006) http://www.time.com/time/2006/techguide/bestinventions/inventions/meals5.html.
76. Guinness World Records (2007) *Guinness World Records 2008*, p.159; Guinness Book: London.
77. Hashimoto, A., Kameoka, T. (1999) Effect of Infrared Irradiation on Drying Characteristics of Wet Porous Materials. *Drying Technology*, 17: 1613.
78. Hashimoto, A., Kameoka, T. (1997) Penetration of Infrared Radiation within a Vegetable Model. *Food Science and Technology, International, Tokyo*, 3: 373.
79. Sawai, J., Nakai, T., Hashimoto, A., Shimizu, M. (2004) A Comparison of the Hydrolysis of Sweet Potato Starch with β-Amylase and Infrared Radiation Allows Prediction of Reducing Sugar Production. *International Journal of Food Science and Technology*, 39: 967.
80. Hashimoto, A., Sawai, J., Igarashi, H., Shimizu, M. (1992) Effect of Far-Infrared Irradiation on Pasteurization of Bacteria Suspended in Liquid Medium below Lethal Temperature. *Journal of Chemical Engineering of Japan*, 25: 275.
81. Hashimoto, A., Igarashi, H., Shimizu, M. (1992) Far-Infrared Irradiation Effect on

Pasteurization of Bacteria on or within Wet-Solid Medium. *Journal of Chemical Engineering of Japan*, 25: 666.

82. Hashimoto, A., Sawai, J., Igarashi, H., Shimizu, M. (1993) Irradiation Power Effect on IR Pasteurization below Lethal Temperature of Bacteria. *Journal of Chemical Engineering of Japan*, 26: 331.
83. Sawai, J., Sagara, K., Kasai, S., Igarashi, H., Hashimoto, A., Kokugan, T., Shimizu, M., Kojima, H. (2000) Far-Infrared Irradiation-induced Injuries to Escherichia coli at Below the Lethal Temperature. *Journal of Industrial Microbiology & Biotechnology*, 24: 19.
84. Sawai, J., Sagara, K., Hashimoto, A., Shimizu, M. (2003) Inactivation of Enzymes and Bacteria by Far-Infrared Radiative Heating. *International Journal of Food Science & Technology*, 38: 661.
85. Mossoba, M. M., Al-Khaldi, S. F., Kirkwood, J., Fry, F. S., Sedman, J., Ismail, A. A. (2005) Printing Microarrays of Bacteria for Identification by Infrared Microspectroscopy. *Vibrational Spectroscopy*, 38: 229.
86. Chan, K. L. A., Kazarian, S. G. (2004) Visualisation of the Heterogeneous Water Sorption in a Pharmaceutical Formulation under Controlled Humidity via FT-IR Imaging. *Vibrational Spectroscopy*, 35: 45.
87. Kazarian, S. G., Chan, K. L. A.(2004) FTIR Imaging of Polymeric Materials under High-Pressure Carbon Dioxide. *Macromolecules*, 37: 579.
88. Gupper, A., Kazarian, S. G. (2005) Study of Solvent Diffusion and Solvent-Induced Crystallization in Syndiotactic Polystyrene Using FT-IR Spectroscopy and Imaging.

Macromolecules, 38: 2327.

89. Green, R. O., Eastwood, M. L., Sarture, C. M., Chrien, T. G., Aronsson, M., Chippendale, B. J., Faust, J. A., Pavri, B. E., Chovit, C. J., Solis, M., Olah, M. R. Williams, O. (1998) Imaging Spectroscopy and the Airborne Visible/Infrared Imaging Spectrometer (AVIRIS). *Remote Sensing Environment*, 65: 227.
90. Asner, G. P., Elmore, A. J., Hughes, R. F., Warner, A. S., Vitousek, P. M. (2005) Ecosystem Structure along Bioclimatic Gradients in Hawai'i from Imaging Spectroscopy. *Remote Sensing Environment*, 96: 497.
91. Smith, A. M. S., Wooster, M. J., Drake, N. A., Dipotso, F. M., Falkowski, M. J., Hudak, A. T. (2005) Testing the Potential of Multi-Spectral Remote Sensing for Retrospectively Estimating Fire Severity in African Savannahs. *Remote Sensing Environment*, 97: 92.
92. Sakai, K. (2001) Terahertz Time-Domain Spectroscopy. *Journal of the Spectroscopical Research of Japan*, 50: 261.
93. Nagel, M., Bolivar, P. H., Brucherseifer, M., Kurz, H., Bosserhoff, A., Büttner, R. (2002) Integrated THz Technology for Label-Free Genetic Diagnostics. *Applied Physics Letters*, 80: 154.
94. Kawase, K., Ito, H. (2002) Application Possibility of Terahertz-Wave Source to Imaging. *Japanese Journal of Radiological Technology*, 58: 441.
95. Watanabe, Y., Kawase, K., Ikari, T., Ito, H., Ishikawa, Y., Minamide, M. Component Analysis of Chemical Mixtures Using Terahertz Spectroscopic Imaging. (2004) *Optics Communications*, 234, 125 (2004).

96. Kawase, K., Watanabe, Y., Ogawa, Y., Ito, H. (2004) Component Spatial Pattern Analysis of Chemicals Using Terahertz Spectroscopic Imaging. *The Transactions of the Institute of Electrical Engineers of Japan. C*, 124: 1339.

97. Hashimoto, A., Kanou, M., Nakanishi, K., Kameoka, T., Ishikawa, Y., Minamide, H., Ito, H., Chaen, H. (2007) Mid-Infrared and THz Spectroscopic Analysis of Mono- and Disaccharides. In *Book of Abstracts of 4th International Conference on Advanced Vibrational Spectroscopy*, p.106.

Captions of Figures

Firure 1. MIR spectra of monosaccharides in aqueous solutions (0.30 M).

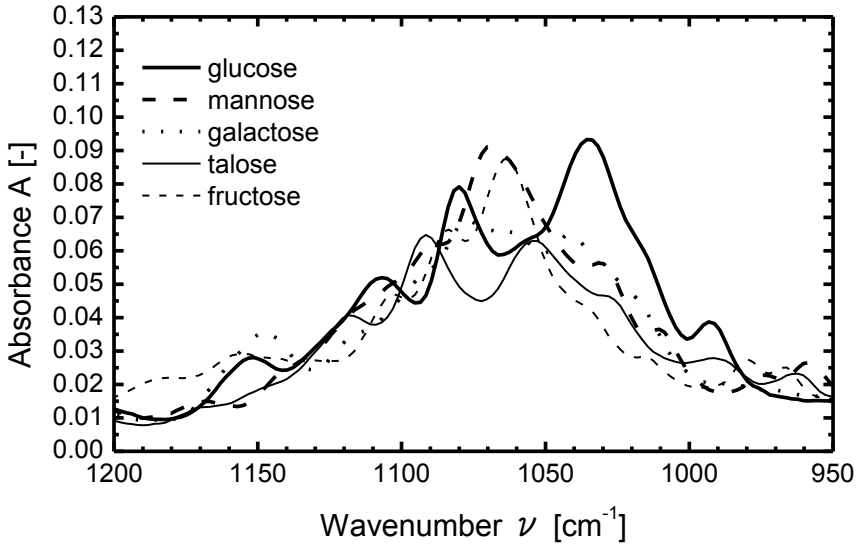

Figure 1

Firure 2. MIR spectra of disaccharides consisting of two glucoses in aqueous solutions (0.15 M).

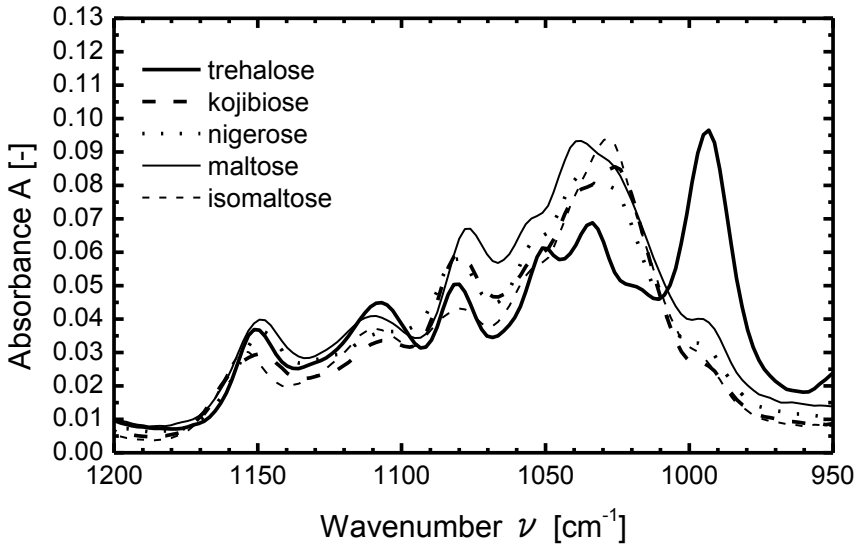

Figure 2

Firure 3. MIR spectra of water and 2.0 M glucose solution with NaCl (NaCl concentration; 0.0 to 4.0 M).

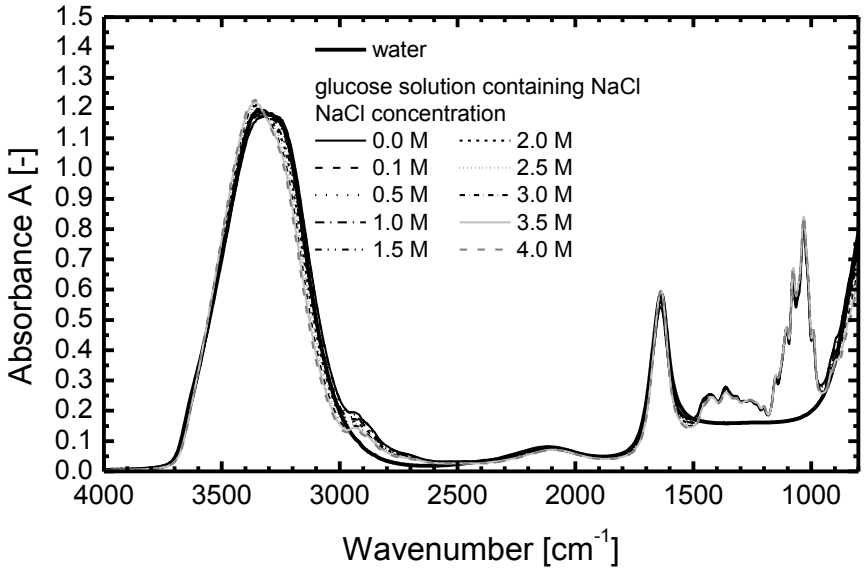

Figure 3

Firure 4. Influence of NaCl concentration on MIR spectra of 2.0 M glucose in aqueous solution with NaCl (NaCl concentration; 0.0 to 4.0 M).

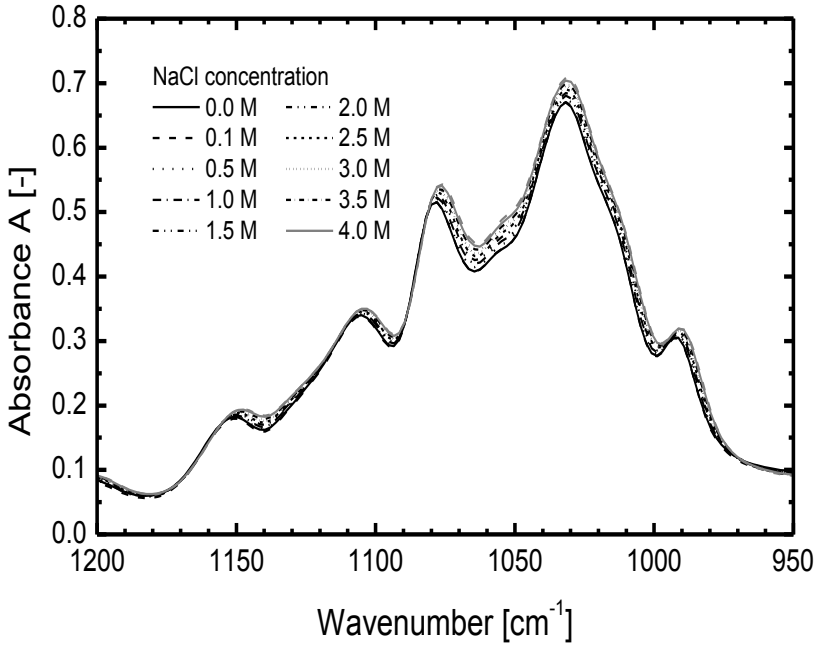

Figure 4

Firure 5. MIR spectral difference between spectrum of glucose in aqueous solution with NaCl (0.0 M) and spectra of those with NaCl (0.1 to 4.0 M).

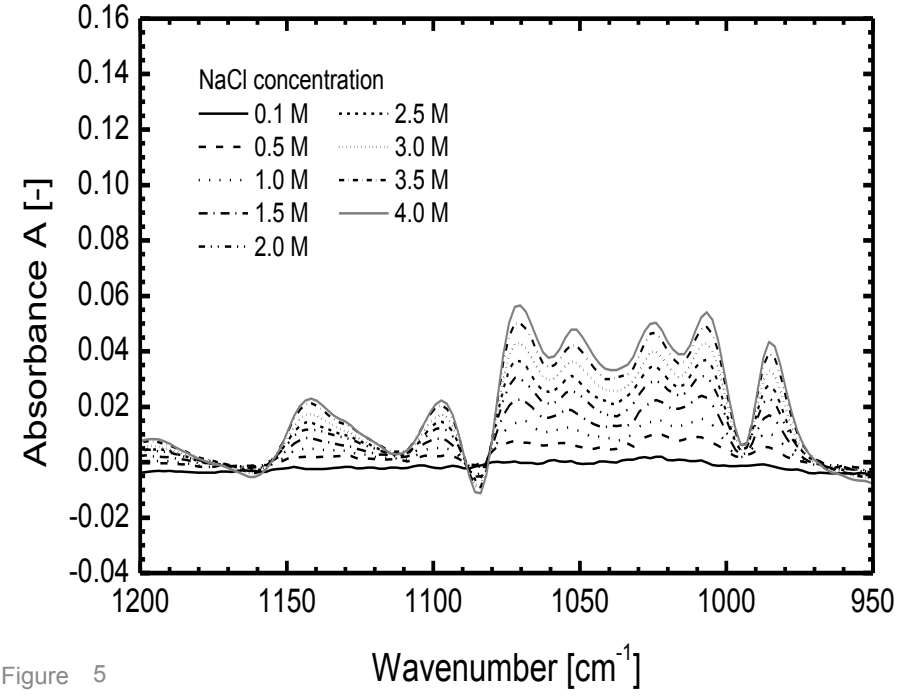

Figure 5

Firure 6. pH-dependency of molar absorbance spectra of G6P.

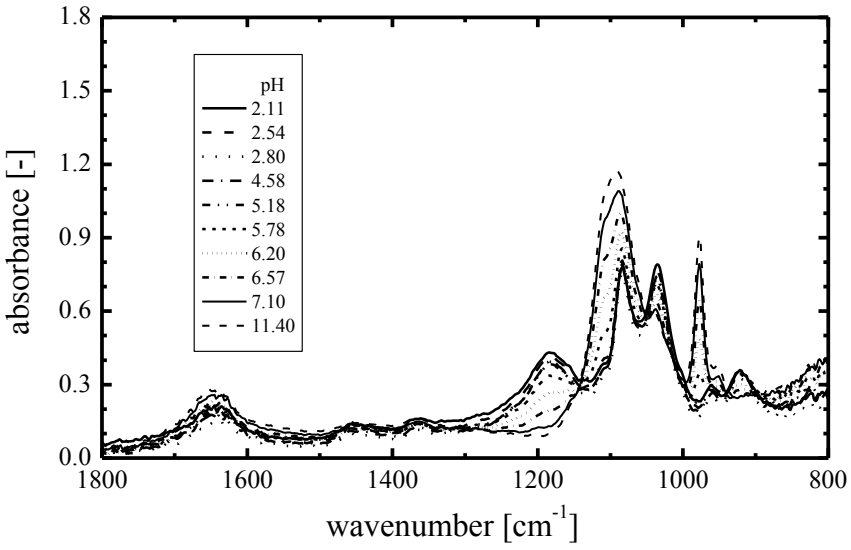

Figure 6

Firure 7. Extracted molar absorbance spectra of ionic species of G6P and corresponding monosaccharide (glucose).

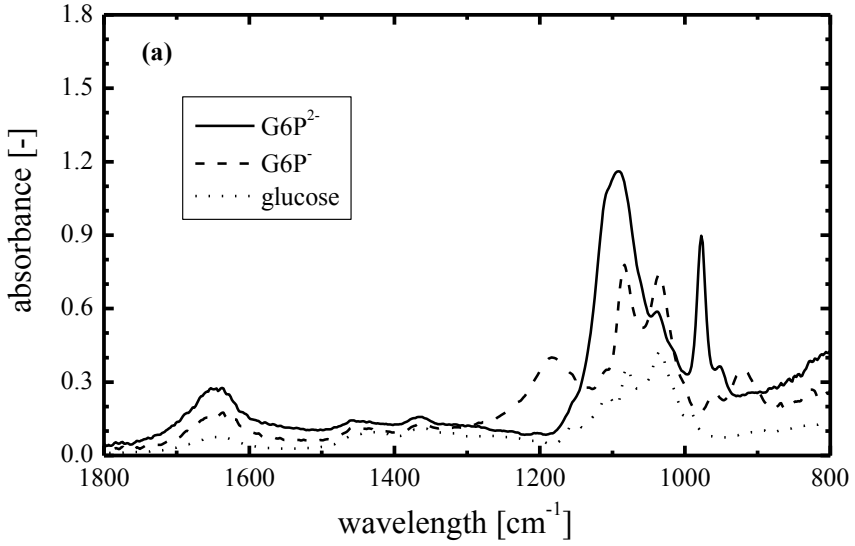

Figure 7

Firure 8. Comparison of the synthesized spectra for G6P at pH 5.78 and 7.10 with the observed spectra.

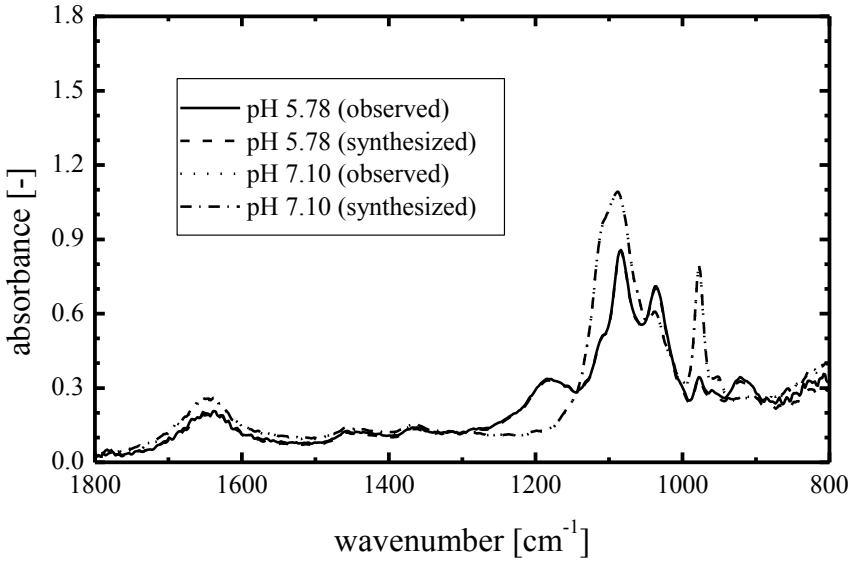

Figure 8

Firure 9. MIR spectra of fresh tomato leaf and the leaf models.

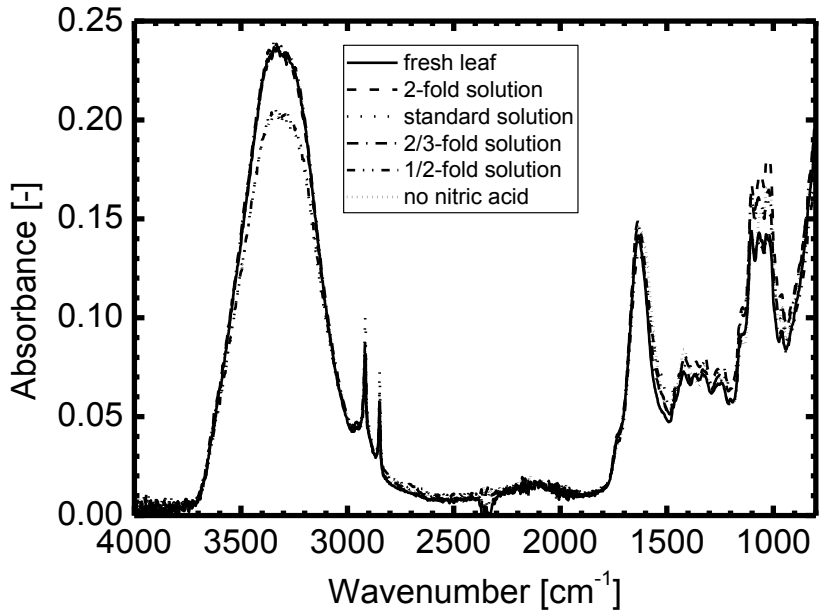

Figure 9

Firure 10. Relationship between absorbance at 1350 cm^{-1} of MIR spectra of leaf model components and nitric acid concentration of nitrogen mixture solution impregnated into leaf model.

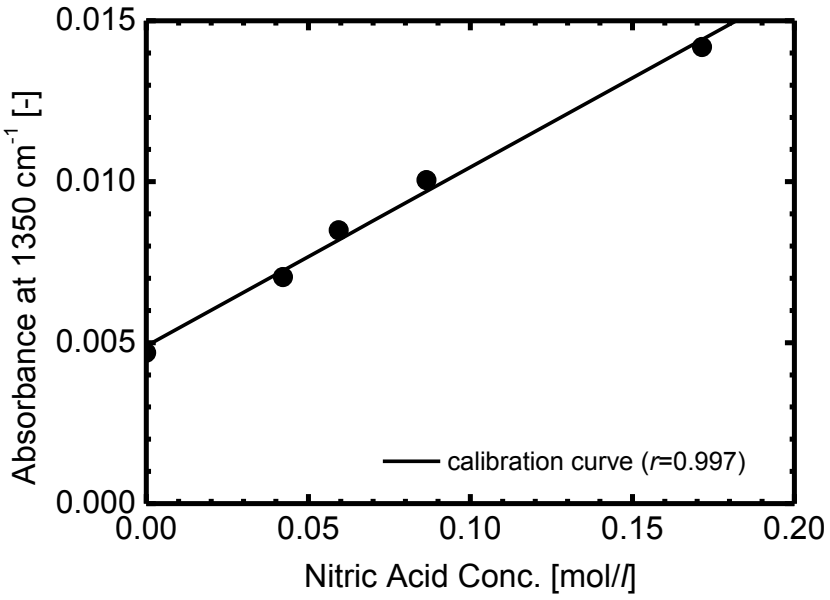

Figure 10

Firure 11. ATR spectra of lettuce leaves of calibrated set: (a) sample in which pesticides residues were detected, (b) sample in which pesticides residues were not detected.

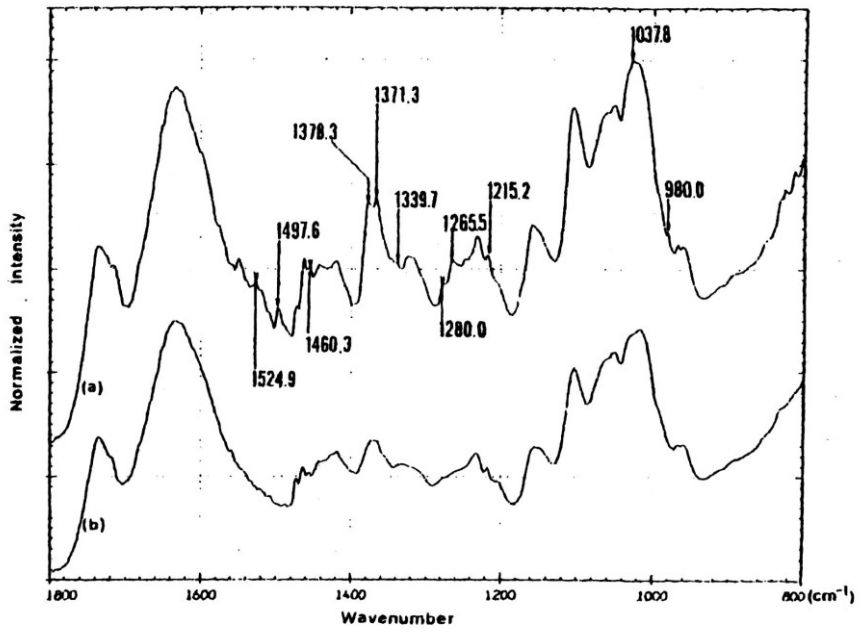

Figure 11

Firure 12. Comparison of the calculated value and actual value: (a) pH value, (b) Tris concentration, (c) G6P concentration, (d) F6P concentration.

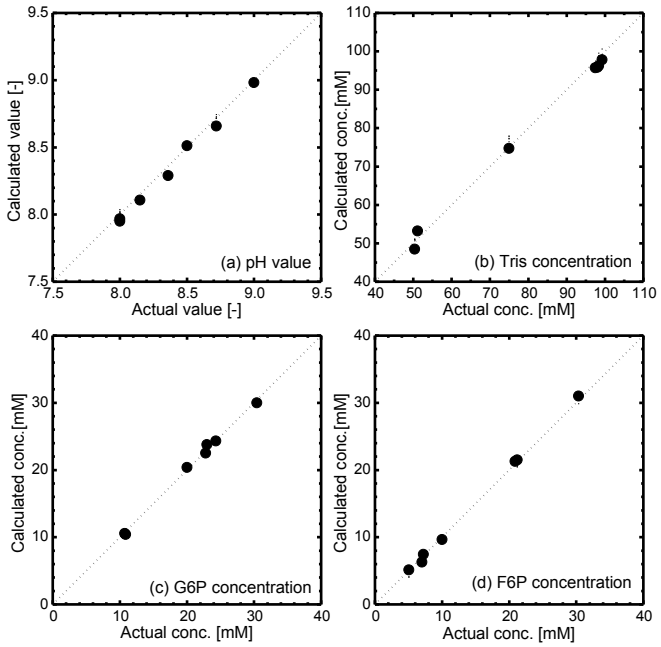

Figure 12

Firure 13. Time changes in reactant spectra.

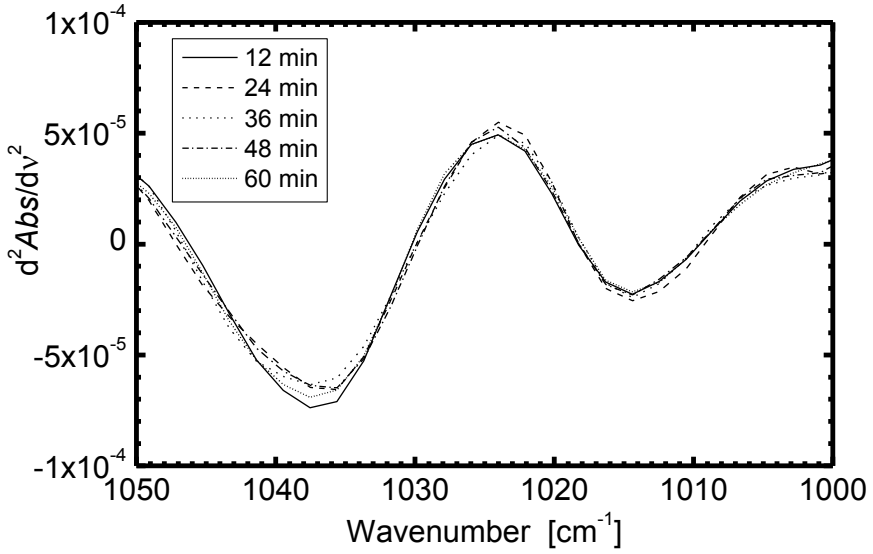

Figure 13

Firure 14. Time courses of metabolite concentration and pH value during enzyme reaction: (a) G6P concentration, (b) F6P concentration, (c) Tris concentration and pH value.

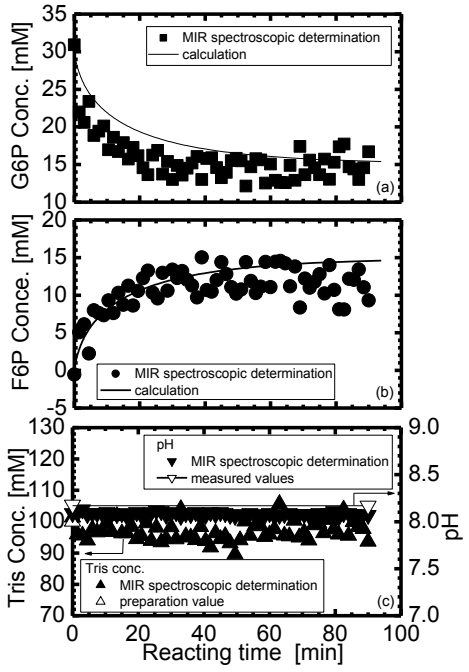

Figure 14

Firure 15. ATR spectra of glucose, fructose, sucrose and ethanol in R2S medium.

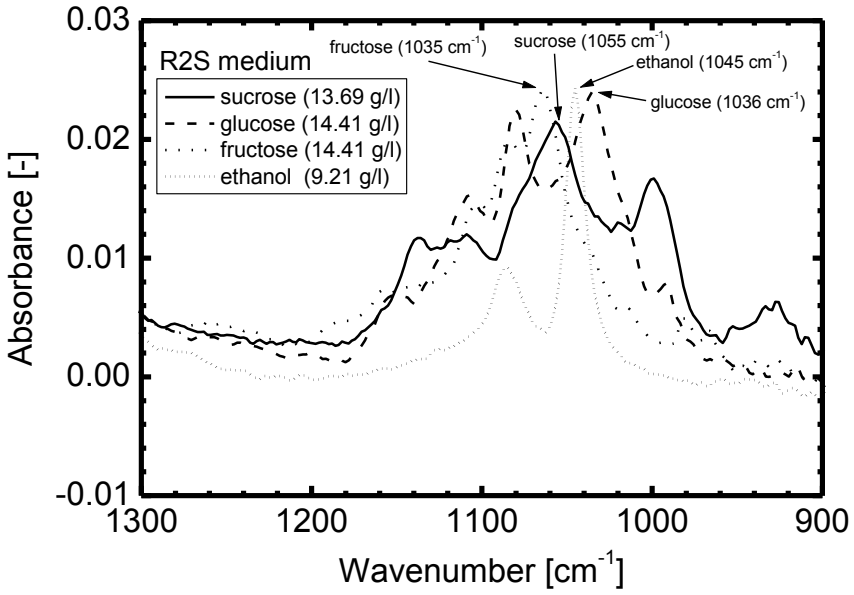

Figure 15

Firure 16. Comparison of sugar and ethanol contents in R2S culture medium during rice cell cultivation evaluated by FT-IR/ATR method with those by HPLC method.

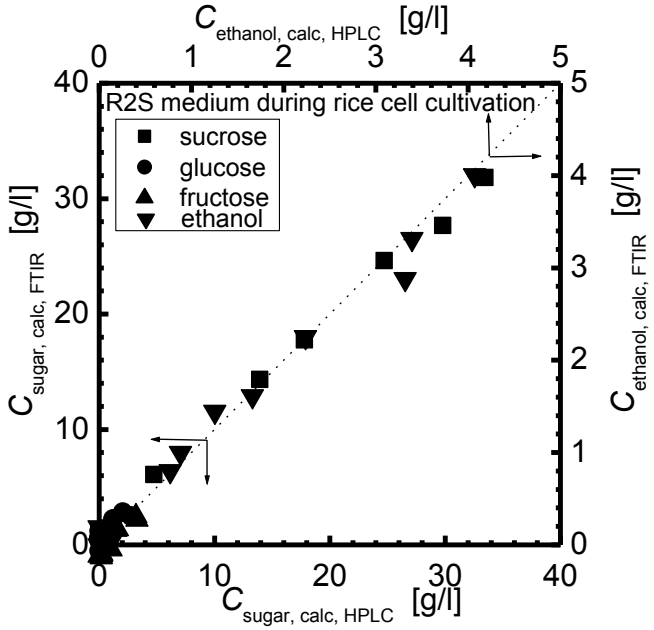

Figure 16

Firure 17. Time behavior of ATR spectra of lactose in yogurt fermentation medium.

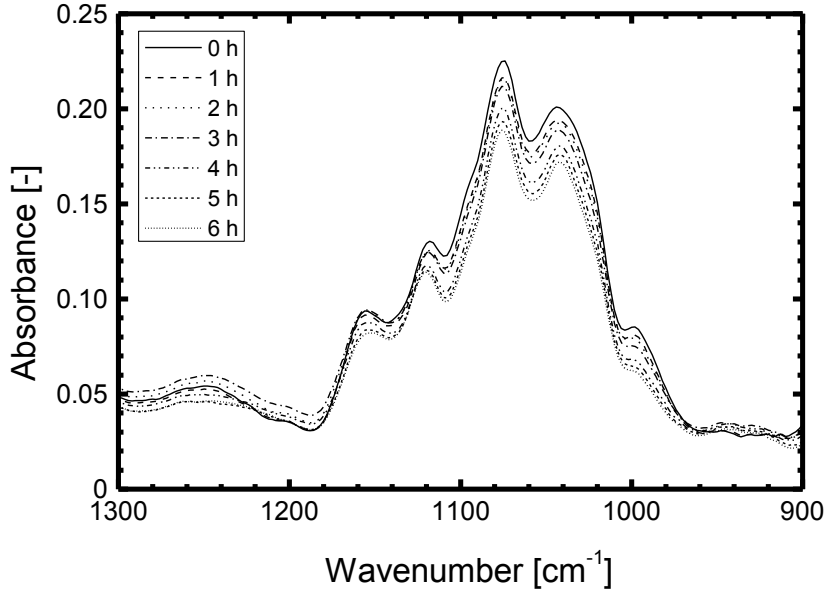

Figure 17

Firure 18. Time behavior of ATR spectra of protein in yogurt fermentation medium.

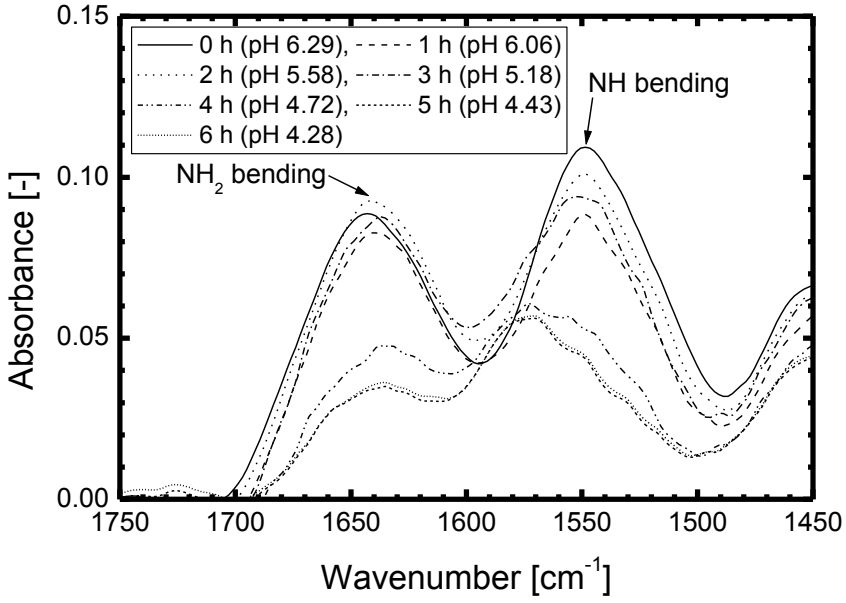

Figure 18

Firure 19. The architecture of the tasting robot.

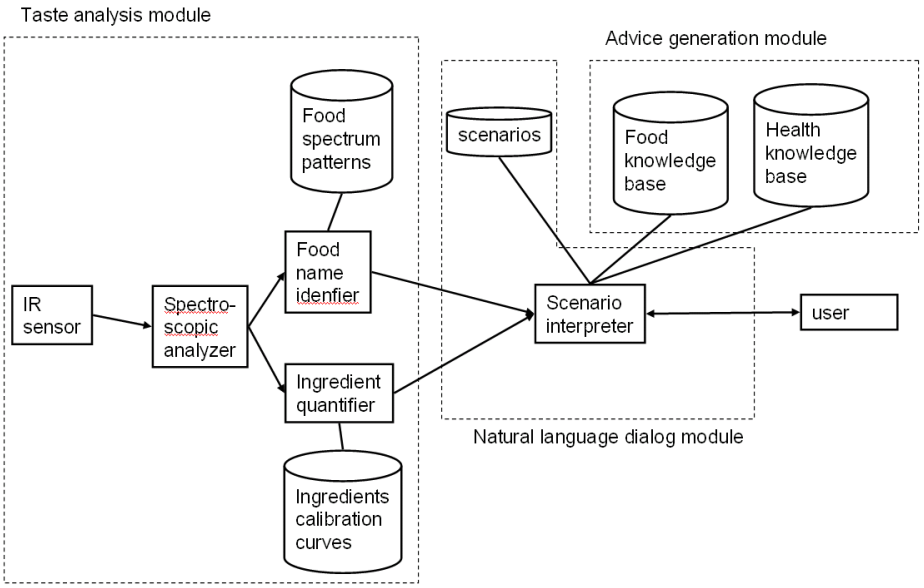

Figure 19

Firure 20. The appearance of the tasting robot.

Figure 20

Firure 21. Scheme of analytical process of spectral information.

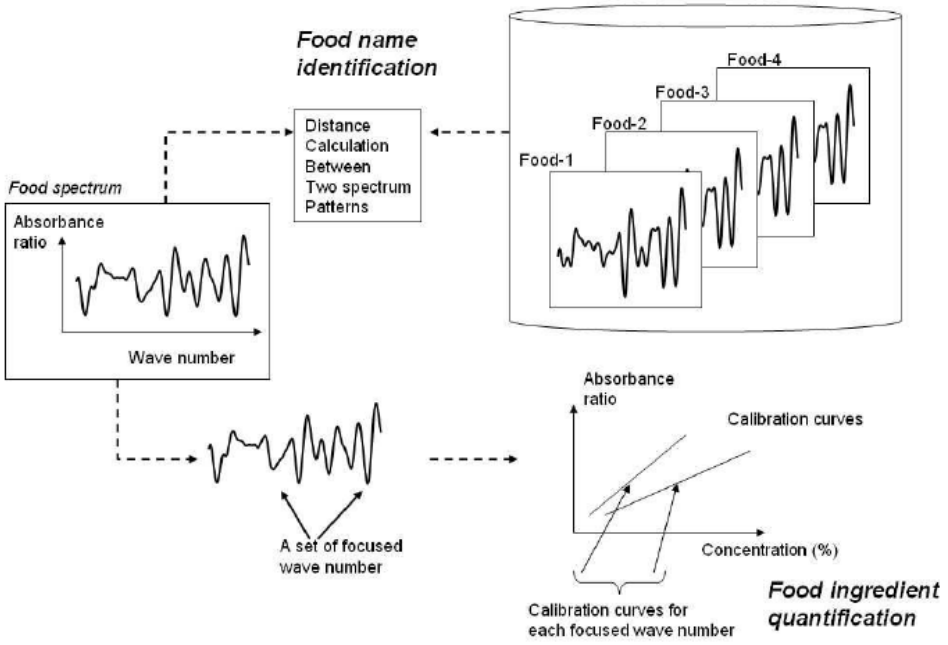

Figure 21

Firure 22. Influences of citric acid concentration on orange juice spectrum characteristics.

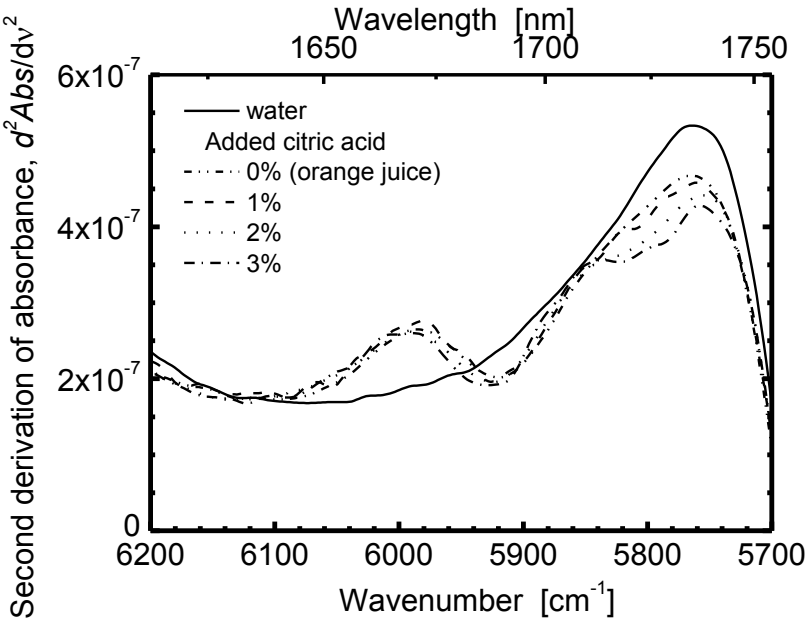

Figure 22

Firure 23. Absorbance spectra of wines.

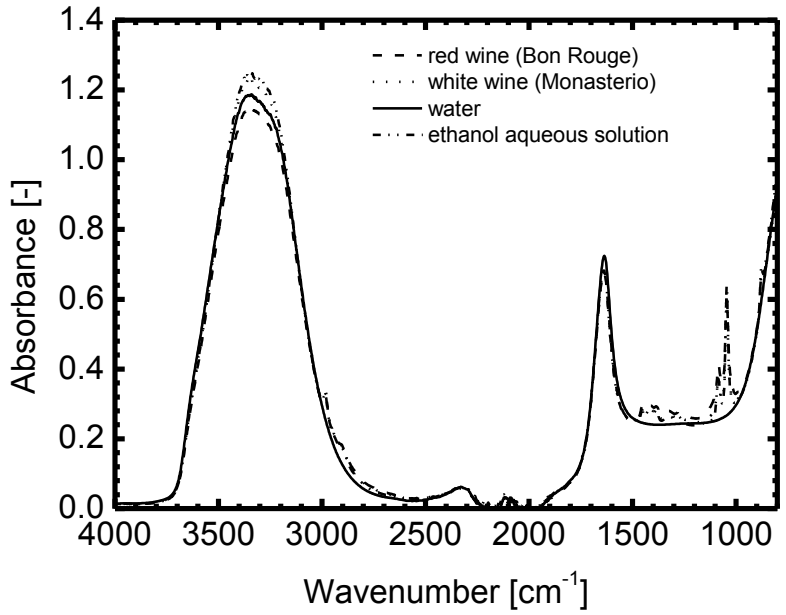

Figure 23

Firure 24. Spectral characteristics of wine components other than ethanol and water.

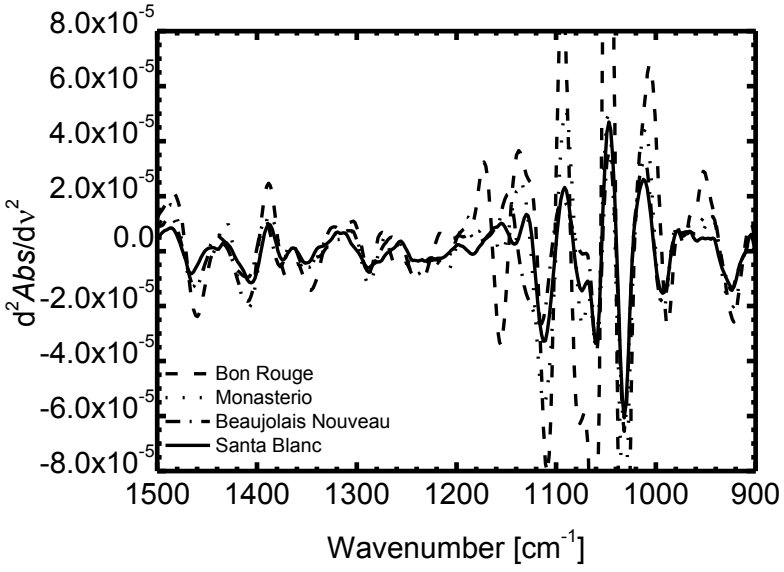

Figure 24